# THE VELOCITY FIELDS IN ECCENTRIC ANNULI

# A THEORETICAL ANALYSIS

# OF THE

# VELOCITY FIELDS

# IN

# ECCENTRIC ANNULI

BY

NORMAN WAYNE WILSON (B. ENG)

A Thesis

Submitted To The Faculty Of Graduate Studies

In Partial Fulfilment Of The Requirements

For The Degree

Master Of Engineering

McMaster University

May 1966

MASTER OF ENGINEERING (1966) McMASTER UNIVERSITY
(Mechanical Engineering) Hamilton, Ontario

TITLE: A Theoretical Analysis Of The Velocity Fields In Eccentric Annuli

AUTHOR: Norman Wayne Wilson, B. Eng. (McMaster University)

SUPERVISOR: Professor J. H. T. Wade

NUMBER OF PAGES: ix, 77

SCOPE AND CONTENTS:

A theoretical analysis of the velocity and wall shear stress distributions for fully developed turbulent flow in annular passages is reported in this thesis. The study was carried out for a range of eccentricities from 0 to 80 percent and for Reynolds numbers from 20,000 to 100,000 for a radius ratio of 1/3.5 with an inner radius of 0.25 inches. For the concentric case, the solution was found to be in agreement with experimental fact.

ACKNOWLEDGEMENTS

The author gratefully acknowledges the assistance and support of Doctor J. H. T. Wade who provided guidance and advice in planning this study. He also extends his appreciation to Doctor J. O. Medwell for his interest in this analysis.

The analytic study reported in this paper was supported financially by National Research Council Grant A-1585.

TABLE OF CONTENTS

## LIST OF FIGURES

## NOMENCLATURE

| SYMBOL | DESCRIPTION |
|---|---|
| **UPPER CASE** | |
| A | AREA |
| $A^+$ | VAN DRIEST'S WALL DAMPING CONSTANT OF TURBULENCE |
| $C_f$ | DIMENSIONLESS WALL SHEAR STRESS $= \frac{\tau_w g_c}{\frac{1}{2} \rho U_m^2}$ |
| $D_H$ | HYDRAULIC DIAMETER OF AN ANNULUS $= 2(r_o - r_i)$ |
| K | UNIVERSAL MIXING CONSTANT |
| L | CHORD LENGTH OF AN ARC |
| P | STATIC PRESSURE |
| Re | REYNOLDS NUMBER $= \frac{U_{av} D_H}{\nu}$ |
| S | ARC LENGTH |
| U | LOCAL TIME MEAN VELOCITY |
| $U^+$ | DIMENSIONLESS VELOCITY $= U/\sqrt{\tau_w g_c/\rho}$ |
| W | COMPLEX POTENTIAL IN THE $\eta, \xi$ PLANE |
| Y | DISTANCE FROM WALL |
| $Y^+$ | DIMENSIONLESS DISTANCE FROM WALL $= \frac{Y\sqrt{\tau_w g_c/\rho}}{\nu}$ |
| Z | COMPLEX POTENTIAL IN THE X-Y PLANE |
| **LOWER CASE** | |
| c | CONSTANT OF ECCENTRIC ANNULAR GEOMETRY |
| d | DISTANCE BETWEEN CENTRES OF AN ECCENTRIC ANNULUS |

| SYMBOL | DESCRIPTION |
|---|---|
| $\frac{dP}{dz}$ | AXIAL PRESSURE GRADIENT |
| f | MOODY FRICTION FACTOR $= 2\frac{g_c D_H}{\rho U_{av}^2} \frac{dP}{dz}$ |
| gc | GRAVITATIONAL CONSTANT |
| r | RADIUS |
| s | RADIUS RATIO $\frac{r}{r_o}$ |
| x | CARTESIAN COORDINATE |
| y | CARTESIAN COORDINATE |
| z | DISTANCE IN AXIAL DIRECTION |

GREEK SYMBOLS

| | |
|---|---|
| $\alpha$ | WALL LOCATION PARAMETER |
| $\beta$ | ANGLE |
| $\epsilon$ | ECCENTRICITY $= \frac{d}{r_o - r_i}$ |
| $\epsilon_m$ | ECCENTRICITY OF APPROXIMATE LINE OF MAXIMUM VELOCITIES $= \frac{dm}{r_o - r_m}$ |
| $\eta$ | ANNULAR COORDINATE |
| $\theta$ | ANGLE |
| $\nu$ | FLUID KINEMATIC VISCOSITY |
| $\xi$ | ANNULAR COORDINATE |
| $\rho$ | FLUID DENSITY |
| $\tau_w$ | WALL SHEAR STRESS |

| SYMBOL | DESCRIPTION |
|---|---|
| SUBSCRIPTS | |
| av | SPATIAL AVERAGE VALUE |
| i | AT OR WITH REFERENCE TO THE INNER WALL |
| l | LAMINAR SOLUTION |
| m | AT THE LINE OF MAXIMUM VELOCITIES |
| o | AT OR WITH REFERENCE TO THE OUTER WALL |
| $\eta$ | $\eta$ = CONSTANT |
| $\xi$ | $\xi$ = CONSTANT |
| 1 | REFERENCED TO POLE OF COMPLEX Z PLANE |
| 2 | REFERENCED TO POLE OF COMPLEX Z PLANE |

## 1. INTRODUCTION

The eccentric annular geometry has many engineering applications such as in heat exchanger and nuclear reactor design. Empirical relationships describing the turbulent flow heat transfer phenomena in eccentric annuli do exist, but to date no satisfactory theoretical analysis has been developed. However, before a solution to this problem can be obtained, the velocity and the fluid stress distributions in the flow field must be thoroughly understood. The present analysis does this by predicting the location of the line of maximum velocities, the velocity field and the shear stress variations on the inner and outer walls of eccentric annuli.

Briefly, the solution was attempted in the following manner. Force balances on incremental areas between the assumed line of maximum velocities and the two walls yielded the local wall shear stresses. These parameters were used in a one dimensional velocity distribution calculated from each wall to obtain two values of the local maximum velocity. The line of maximum velocities was then shifted until these values were equal.

By repeating this procedure for successive incremental areas, the velocity and wall shear stress distributions were found for the complete flow field.

Because of the lengthy nature of the solution, the analysis was performed numerically on an IBM 7040 computer. The final results were then correlated in dimensionless form and presented graphically for a wide range of eccentricities and Reynolds numbers.

## 2. LITERATURE SURVEY

One of the attempts at a solution for the turbulent flow velocity profiles in eccentric annuli was developed by Heyda (1)[1]. The orthogonal co-ordinate system consistent with the boundaries of an eccentric annulus was developed as part of the solution for point velocities in the laminar flow field of an annulus. The location of the line of maximum velocities was found by setting $\frac{\partial U}{\partial \eta} = 0$ in the solution for the laminar case and a simplified approximate equation was determined for this location. Heyda then assumed that the line of maximum velocities for turbulent flow coincides with that for laminar flow. Assuming, in effect, that the wall shear stresses were constant over each boundary, a force balance was performed on the area bounded by the wall in question and the line of maximum velocities to determine the boundary shear stress. An iterative procedure was used to determine the correct shear stresses at the wall and hence the pressure gradient in the axial direction for a given average velocity .

The velocity profile suggested by Heyda was that due to Van Driest (2) who has developed a continuous velocity profile describing the sublayer, the transition region and the turbulent core by considering the damping effect of the wall on simple harmonic fluid oscillations. This profile was

1. ( ) indicates references listed in Section 8.

derived for fully developed flow over a flat plate but a favourable comparison was made by Van Driest with experimental results for pipe flow. For the sublayer the profile approached the accepted relation

$$U^+ = Y^+$$

The outer region of the profile approached the relation

$$U^+ = \frac{1}{K} \ln Y^+ + C$$

which is the universal velocity distribution due to Prandtl.

In Heyda's paper the distances from the walls were calculated along lines which were members of the family orthogonal to the walls. In essence, Heyda has assumed that the geometry of the flow field is the governing factor for the application of the velocity profile law. (A further discussion of this problem is presented in Section 4).

Although a note in Heyda's paper stated that a preliminary programme had been written, no information could be found to establish the general validity of his solution. However, a review of his assumptions shows that an extension of his work is in order. Since an eccentric annulus is a two dimensional flow field rather than one which is axisymmetric, a shear stress variation around

both the inner and outer walls would be expected. His further assumption that the line of maximum velocities for the turbulent flow case coincides with that for laminar flow is not necessarily valid. These two assumptions are more realistically dealt with in the present analysis.

Deissler and Taylor (3,4) have generalized their previous analysis of flow in tubes to apply in an annulus. An initial estimate of the location of lines of constant velocity was made to facilitate sketching the velocity gradient lines orthogonal to the constant velocity lines shown in Figure 4. Values of the local wall shear stress were determined by performing force balances on the area bounded by the wall in question and two adjacent velocity gradient lines. As a result of these calculations a new set of constant velocity lines were then obtained using straight lines normal to the wall midway between the previous velocity gradient lines as wall distance parameters in a set of equations describing a generalized velocity distribution for fully developed turbulent flow in smooth tubes.

Deissler and Taylor's choice of wall distance parameters is considered in depth in Section 4. The only locations where this choice is fully apparent are at the lines describing maximum and minimum separation. As the

authors have pointed out, some difficulty in obtaining orthogonality of the constant velocity lines and velocity gradient lines was experienced in cases of high eccentricity. This may have been caused by the choice of straight lines normal to the walls as distance parameters.

There is little or no experimental data available to substantiate Heyda's or Deissler and Taylor's analyses. However, sufficient reliable information exists for the case of zero eccentricity in turbulent flow. This work is briefly reviewed so that a partial comparison to the foregoing analyses may be made.

Two separate investigations were conducted by Brighton and Jones (5) and Ivey (6) for radius ratios from .0625 to .7 and over a Reynolds number range of 10,000 to 327,000. Particular attention was paid to finding the location of the point of maximum velocity. Both investigators found that the location was nearer the inner wall than for laminar flow, the deviation being greatest for small radius ratios. It was found that the location was virtually independent of Reynolds number and the hydraulic diameter of the annuli. Heyda's assumption of coincidence of the location of the line of maximum velocities in the laminar and turbulent cases is, therefore, unjustifiable. Deissler and Taylor's analysis was carried

out for one radius ratio only; however, their friction factor evaluation for a radius ratio of $\frac{1}{3.5}$ was in agreement with Brighton and Jones' findings.

## 3. ANALYSIS

Before the boundary shear stress distribution and the velocity field may be determined, the plane geometry of the flow field must be described by a suitable co-ordinate system. Such a system requires that lines along which a velocity distribution is assumed to apply are orthogonal to both the inner and outer walls. To facilitate this, Heyda developed the ( $\eta$ , $\xi$ ) coordinate system with respect to ordinary Cartesian coordinates with an origin on the common annular diameter to the right of the outer wall. The $\eta$ coordinate family, which defines the inner and outer walls, consists of a set of circles with centres along the negative x-axis, and the $\xi$ family, orthogonal to the $\eta$ family, is a set of circles with centres along the y-axis (cf Figure 1). The development of the ($\eta$, $\xi$ ) system is reviewed in detail in the Appendix (Section 7.1), and the justification for adopting this system in the present analysis is discussed in Section 4.

With the field geometry specified, a force balance may be performed on a fluid element between the boundaries and the line of maximum velocities to determine the variation of the wall shear stresses. This information

may be used in a form of the Van Driest profile to obtain the velocity field. It is convenient to describe the annular geometry in $(\eta, \xi)$ coordinates as shown in Figure 1.

For an inner radius, $r_i$, an outer radius, $r_o$, and an eccentricity, $\epsilon$, the outer and inner boundaries are described by $\eta_o$ and $\eta_i$ which are given by

$$\eta_o = \cosh^{-1}\left(\frac{1}{2}\left[\frac{1+S}{\epsilon} - (1-S)\epsilon\right]\right) , \qquad (1)$$

and

$$\eta_i = \sinh^{-1}\left(\frac{c}{r_i}\right) \qquad (2)$$

where $$S = \frac{r_i}{r_o} , \qquad (3)$$

and $$c = r_o \sinh \eta_o . \qquad (4)$$

Heyda approximated the location of the line of maximum velocities for laminar flow by

$$\eta_{ml} = \operatorname{sech}^{-1}\frac{1}{2}\left(\sqrt{(1-\tanh\eta_i)(1+\tanh\eta_o)} + \sqrt{(1+\tanh\eta_i)(1-\tanh\eta_o)}\right). \qquad (5)$$

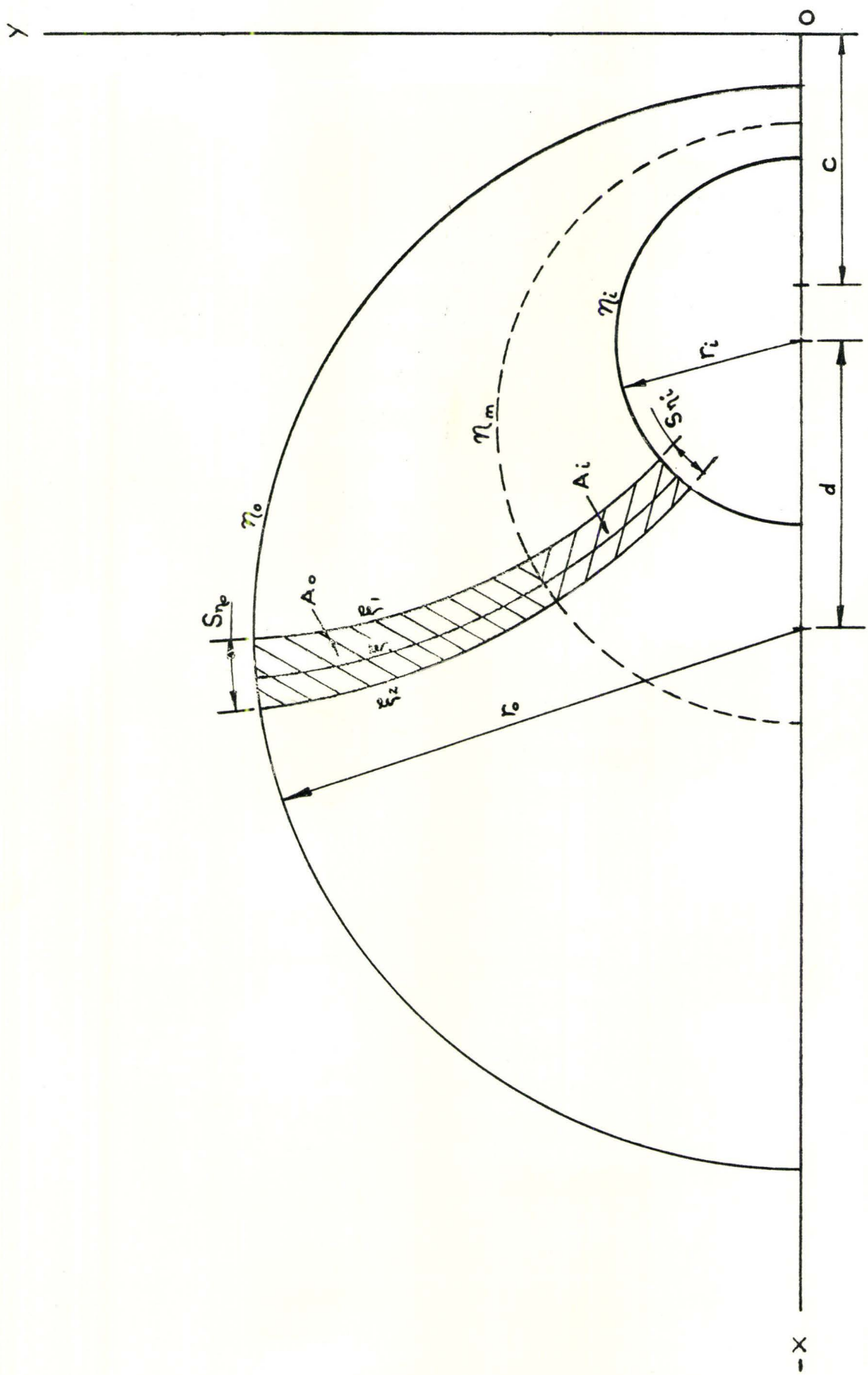


FIGURE I GEOMETRY OF AN ANNULUS

This equation will be used as a first approximation in the present analysis.

Noting that $\xi_1$ and $\xi_2$, shown in Figure 1, are determined as

$$\xi_1 = \xi - \frac{\Delta\xi}{2} \quad , \tag{6}$$

and

$$\xi_2 = \xi + \frac{\Delta\xi}{2} \quad . \tag{7}$$

the incremental areas, $A_i$ and $A_o$, identified by a particular value of $\xi$, are given by

$$A_i = -c^2 \int_{\eta_i}^{\eta_m} \int_{\xi_1}^{\xi_2} \frac{d\eta\, d\xi}{(\cosh\eta + \cos\xi)^2} \quad , \tag{8}$$

and

$$A_o = -c^2 \int_{\eta_m}^{\eta_o} \int_{\xi_1}^{\xi_2} \frac{d\eta\, d\xi}{(\cosh\eta + \cos\xi)^2} \quad . \tag{9}$$

The $(\eta, \xi)$ coordinates of any point may be transformed to Cartesian coordinates by means of the equations

$$x = \frac{-c \sinh\eta}{\cosh\eta + \cos\xi} \quad , \tag{10}$$

and $$y = \frac{c \sin \xi}{\cosh \eta + \cos \xi} \tag{11}$$

These equations allow the chord length, $L_\eta$, between two points at $(\eta, \xi_1)$ and $(\eta, \xi_2)$ to be determined as

$$L_\eta = \left\{ \left( x(\eta, \xi_1) - x(\eta, \xi_2) \right)^2 + \left( y(\eta, \xi_1) - y(\eta, \xi_2) \right)^2 \right\}^{1/2} . \tag{12}$$

Similarly, the chord length, $L_\xi$, between two points on a line of constant $\xi$ may be calculated.

As developed in the Appendix the arc lengths around the inner and outer walls between $\xi_1$ and $\xi_2$ are

$$S_{\eta_i} = \frac{2c}{\sinh \eta_i} \sin^{-1} \left\{ \frac{L_{\eta_i} \sinh \eta_i}{2c} \right\} , \tag{13}$$

and $$S_{\eta_o} = \frac{2c}{\sinh \eta_o} \sin^{-1} \left\{ \frac{L_{\eta_o} \sinh \eta_o}{2c} \right\} . \tag{14}$$

Similarly arc lengths along constant $\xi$ lines from the inner or outer wall, as the case may be, are determined by

$$S_{\xi_i} = \frac{2c}{\sin \xi} \sin^{-1} \left\{ \frac{L_{\xi_i} \sin \xi}{2c} \right\} \tag{15}$$

for the inner region, and

$$S_{\xi_o} = \frac{2c}{\sin \xi} \sin^{-1} \left\{ \frac{L_{\xi_o} \sin \xi}{2c} \right\} \tag{16}$$

for the outer region.

With the important aspects of the field geometry completed, the forces acting on an element of fluid of unit axial length and cross sectional area $A_i$ may be considered for fully developed turbulent flow. In this case $\frac{dP}{dz}$ is constant over the flow area. Since ideally the line of maximum velocities describes locations where $\frac{\partial U}{\partial \eta} = 0$, the shear stress at these locations may be assumed to be zero. If the net effect of the fluid shear acting on the faces $\xi_1$ and $\xi_2$ is negligible and the wall shear stress $\tau_{wi}$ is assumed constant over the incremental face $S_{\eta i}$, a force balance on the element will yield

$$\tau_{wi} S_{\eta i} = \frac{dP}{dz} A_i \quad ,$$

or

$$\tau_{wi} = \frac{dP}{dz} \frac{A_i}{S_{\eta i}} \quad . \tag{17}$$

A similar treatment of the outer element of fluid will yield

$$\tau_{wo} = \frac{dP}{dz} \frac{A_o}{S_{\eta o}} \quad . \tag{18}$$

These two equations may be used to determine the shear velocities, $\sqrt{\frac{\tau_w g_c}{\rho}}$, required for the Van Driest profile which is assumed to apply along lines of constant $\xi$. The arc length from the wall in question may be used as a wall distance parameter. In this case the dimensionless velocities and distances for use in the profile are given for the inner region ($\eta_m \leq \eta \leq \eta_i$) as

$$U^+ = \frac{U}{\sqrt{\frac{\tau_{wi} g_c}{\rho}}} \quad , \tag{19}$$

and

$$Y^+ = \frac{S_{\xi i} \sqrt{\frac{\tau_{wi} g_c}{\rho}}}{\nu} \quad . \tag{20}$$

for the outer region ($\eta_o \leq \eta \leq \eta_m$), they are given by

$$U^+ = \frac{U}{\sqrt{\frac{\tau_{wo} g_c}{\rho}}} \quad , \tag{21}$$

and

$$Y^+ = \frac{S_{\xi o} \sqrt{\frac{\tau_{wo} g_c}{\rho}}}{\nu} \quad . \tag{22}$$

These quantities are related in the Van Driest velocity distribution, shown in Figure 2, in the following manner:

$$U^+ = \int_0^{Y^+} \frac{2\, dY^+}{1 + \sqrt{1 + 4K^2 Y^{+2} \{1 - \exp(-Y^+/A^+)\}^2}} \quad , \tag{23}$$

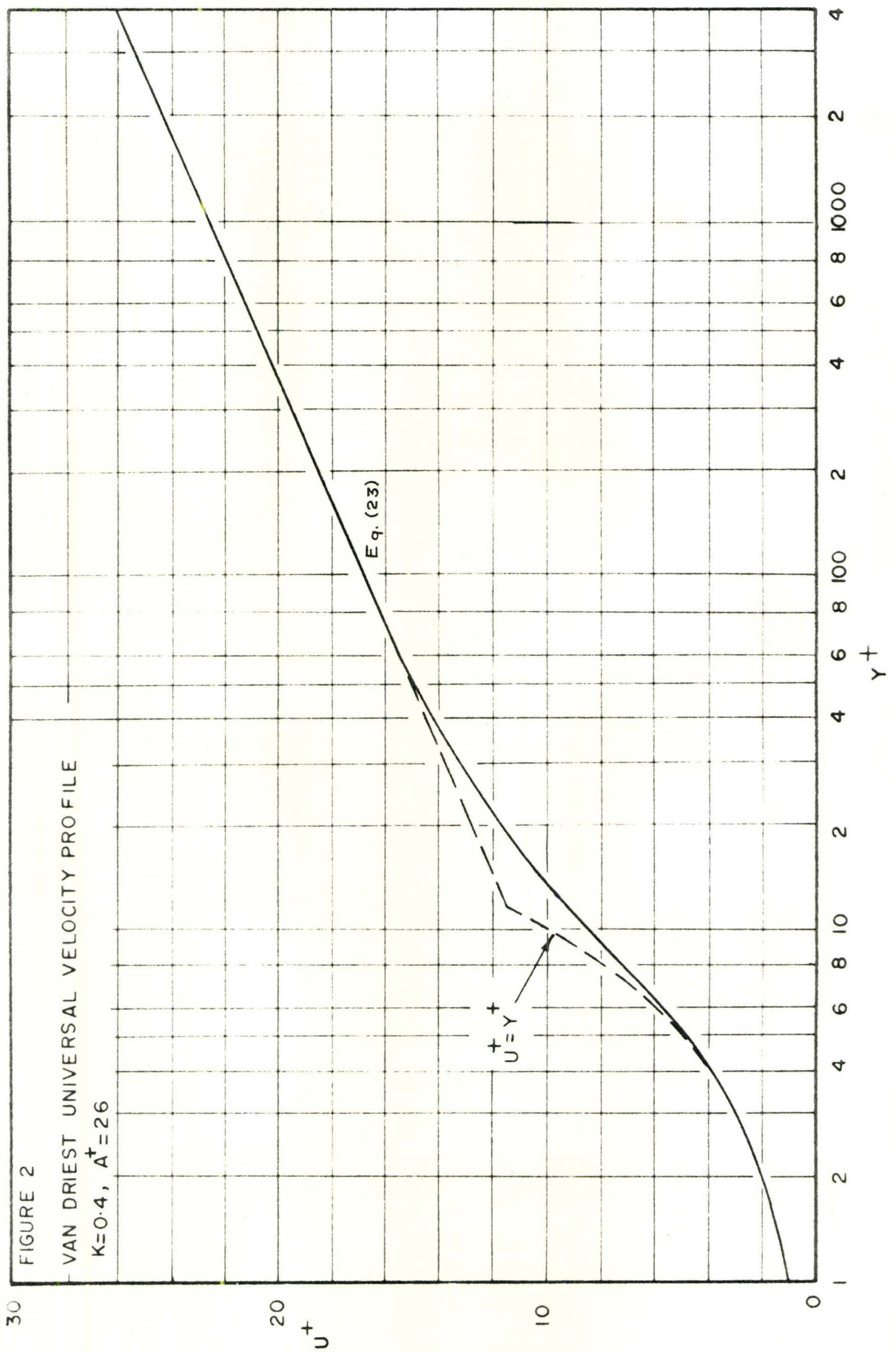
FIGURE 2
VAN DRIEST UNIVERSAL VELOCITY PROFILE
K=0·4, A+=26
Eq. (23)
U+=Y+
U+
Y+
0
10
20
30
1
2
4
6
8
10
2
4
6
8
100
2
4
6
8
1000
2
4

where the values K = 0.4 and $A^+$ = 26 are as suggested by Van Driest. At the line of maximum velocities it is possible to calculate two values of velocity. One is referred to the inner wall and the other to the outer wall. Thus, the condition that these two velocities must agree may be used to determine the correct location of the line of maximum velocities by shifting $\eta_m$ in a trial and error procedure and recalculating the wall shears for the new location of $\eta_m$. A consideration of successive values of $\xi$ around the flow area then permits the calculation of the entire velocity field.

The average velocity of the flow field is evaluated by integrating the point velocities over the area. Thus

$$U_{av} = \left( \int_A U \, dA \right) / A \quad . \tag{24}$$

$$\int_A U \, dA = -2c^2 \left( \int_{\eta_i}^{\eta_m} \int_0^{\pi} \frac{U(\eta, \xi) \, d\eta \, d\xi}{(\cosh \eta + \cos \xi)^2} + \int_{\eta_m}^{\eta_o} \int_0^{\pi} \frac{U(\eta, \xi) \, d\eta \, d\xi}{(\cosh \eta + \cos \xi)^2} \right) , \tag{25}$$

and $$A = \pi ( r_o^2 - r_i^2 ) \quad . \tag{26}$$

Based on the hydraulic diameter $D_H$, the Reynolds number is defined as

$$R_e = \frac{U_{av} D_H}{\nu} \quad . \tag{27}$$

For an annulus

$$D_H = 2 ( r_o - r_i ) \quad . \tag{28}$$

This information is used to determine a dimensionless average shear stress - Reynolds number relationship.

It is apparent that the complete solution requires the application of the foregoing equations to a large number of finite sections of the flow field. The Van Driest profile and the area integrations must be evaluated several times for each value of $\xi$ chosen because of the trial and error method of locating the line of maximum velocities. Consequently, the solution was programmed for an IBM 7040 computer. This solution in FORTRAN IV language is shown in detail in the Appendix (Section 7.2).

## 4. DISCUSSION OF THE FIELD GEOMETRY

Before the results of the analysis are presented, the compatibility of the choice of the field geometry with the velocity distribution will be re-examined. This is best done by first considering two familiar cases.

For fully developed flow over a flat plate or in a circular pipe, simple coordinate systems conveniently describe the velocity field. In the first case, the Cartesian coordinate system defines the lines of constant velocity and the orthogonal lines which are, by definition, velocity gradient lines. Figure 3, a graphical presentation of flow over a flat plate, shows that one set of the coordinate lines, the velocity gradient lines, and the edge views of the profile curves are inseparable in this simple flow geometry. The same concept applies to flow in a circular pipe. Constant velocity lines, which are a set of concentric circles, and velocity gradient lines, a set of radii, are described by the polar coordinate system. In both of these cases, edge views of the velocity profiles are identical with the coordinate lines normal to the walls. However, in the application of accepted velocity distributions to the eccentric annular configuration, this simplicity does not exist.

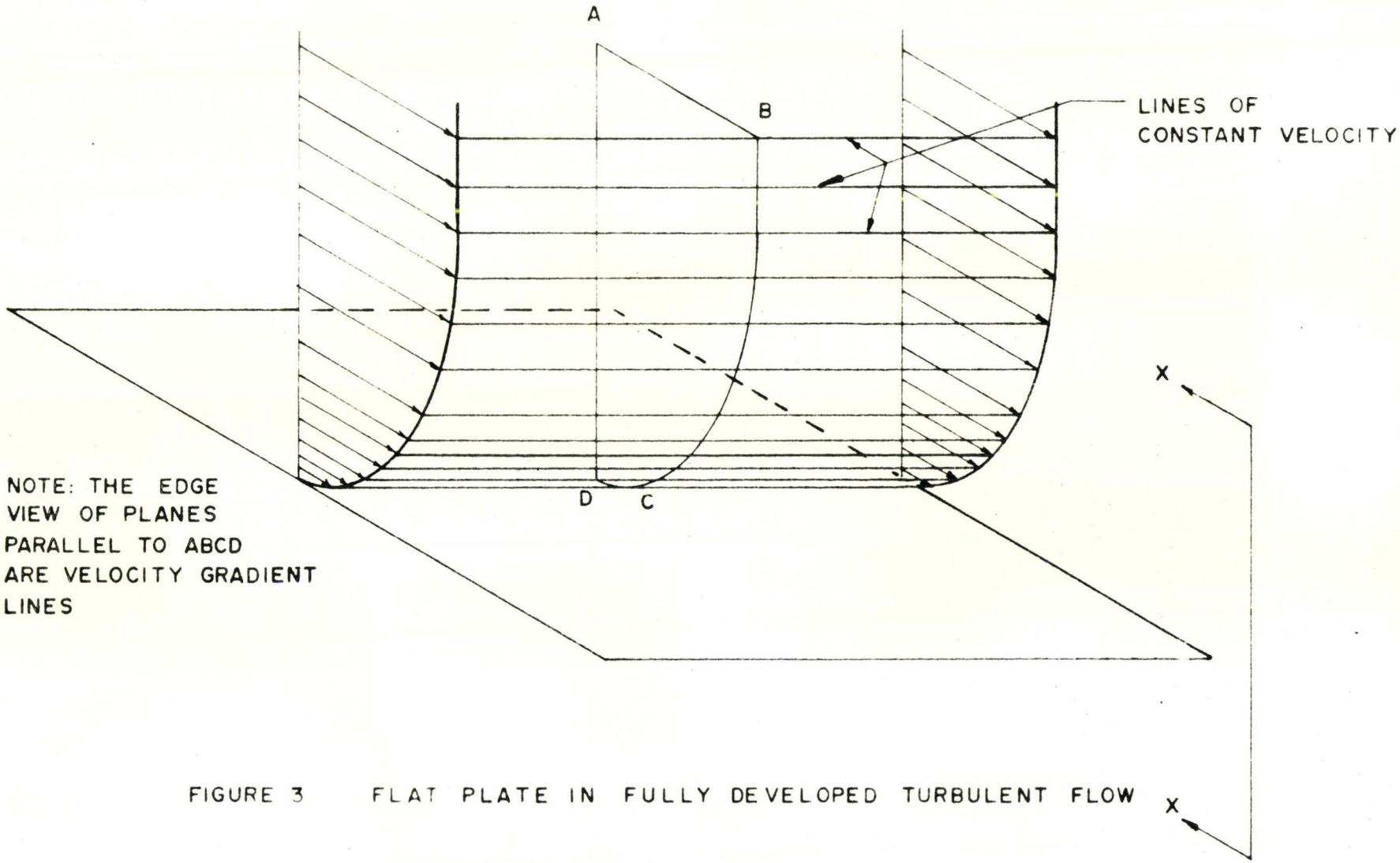


FIGURE 3 FLAT PLATE IN FULLY DEVELOPED TURBULENT FLOW

Intuitively, the flow field in this case is expected to be similar to that determined by Deissler and Taylor. Figure 4 shows the lines of constant velocity made dimensionless with respect to the average velocity for a range from 1.36 to 0.40. The broken lines are velocity gradient lines which by definition are orthogonal to the constant velocity lines. Deissler and Taylor assumed that the velocity profile applied along the straight solid lines perpendicular to the inner and outer walls. However, since these lines are not normal to the line of maximum velocities, a component of velocity gradient would be resolved along them from the gradient existing along the line of maximum velocities. This would manifest itself in a relatively large slope of the velocity profile at the point of maximum velocity.

In Heyda's analysis this problem is diminished by choosing the constant $\xi$ lines (see Figure 1), which are very nearly orthogonal to the line of maximum velocities, for application of the Van Driest distribution. Two of the $\eta$ coordinates describe lines of zero velocity corresponding to the two boundaries and are orthogonal to the $\xi$ coordinates. Since the $(\eta, \xi)$ coordinate system satisfies the requirements of orthogonality, it is justifiably adopted for the present analysis. A further advantage is that this system is formulated mathematically and is, therefore,

FIGURE 4

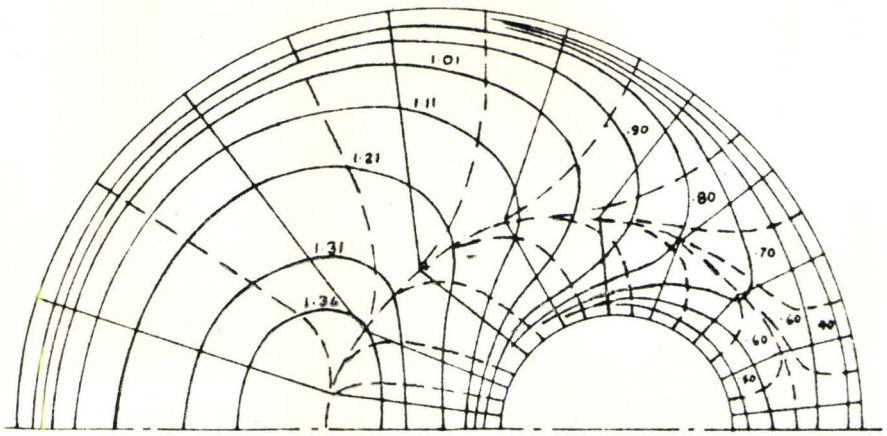


CONSTANT VELOCITY MAP DUE TO DEISSLER & TAYLOR SHOWING $U/U_{av}$ FOR S=1/3·5 & ECCENTRICITY=60%

readily adapted to a machine solution.

## 5. DISCUSSION OF RESULTS

The equations were solved with the aid of the computer programme developed in Section 7.2 for five eccentricities at Reynolds numbers up to 100,000 for a radius ratio of 1/3.5.

The velocity fields are first considered by mapping the lines of constant velocity on the cross section of the flow area. A typical mapping is shown in Figure 5 where the lines of constant velocity have been made dimensionless with respect to the average velocity. Where the velocity lines cross the line of maximum velocities, a discontinuity in shape occurs at the point of intersection. This is due to the finite slope of the Van Driest profile at the position of maximum velocity. Generally, however, the constant velocity lines indicate that the highest velocities, and hence the largest percentage of the flow per unit area, occur in the region where the separation of the boundaries is the greatest, and that the velocities and flow rates decrease to a minimum at the narrowest section of the flow field.

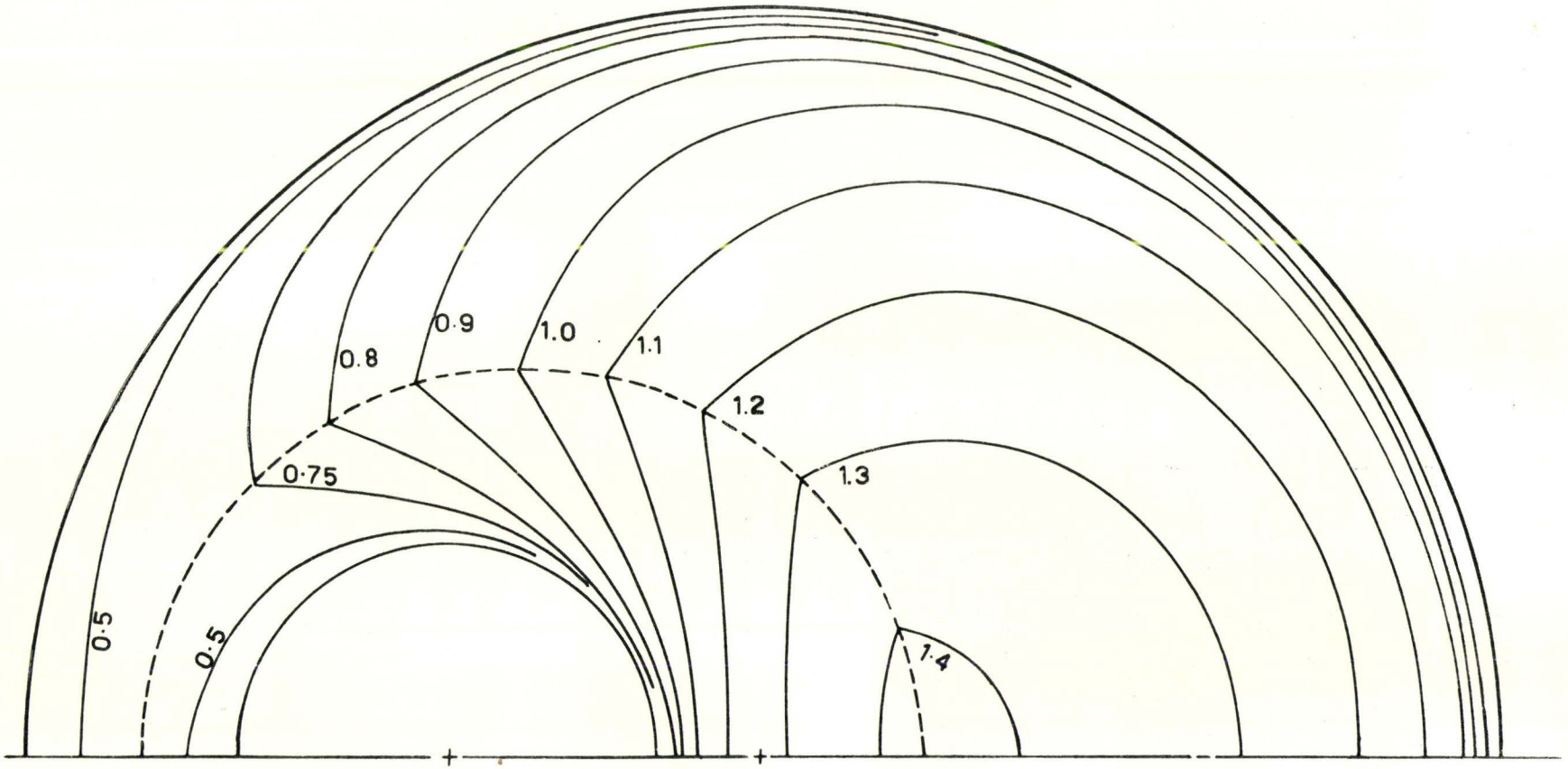


FIGURE 5 TYPICAL MAPPING OF LINES OF CONSTANT $U/U_{av}$

Re=21,000, $r_i$ =·25, $r_o$ =·875, $\epsilon$ =·60

An indication of this decrease is shown in Figure 6 where the variation of the velocity along the line of maximum velocities is plotted against an outer wall location parameter. (The actual parameter, $\alpha_o$, is defined and related to a corresponding inner wall location, $\alpha_i$, in Figure 7 with both parameters being measured from the point of minimum separation). The slight lowering of values of Um/Uav for increased Reynolds numbers is attributed to the flattening of the velocity distribution. In the region of minimum separation in the 80% eccentric case, the reversal of this trend is caused by the small radius of curvature of the inner wall and the steep gradient along the line of maximum velocities.

Of equal importance to the maximum velocity distribution is the location and shape of the line along which this variation exists. Figure 8 shows that the $\eta$ coordinates of the line of maximum velocities are independent of Reynolds number and very nearly constant through the field for each eccentricity. Thus, it is possible to describe these lines approximately by circles which are eccentric with respect to the outer wall. The radius and eccentricity of such circles are given in Figures 9 and 10 as functions of the annulus eccentricity

FIGURE 6

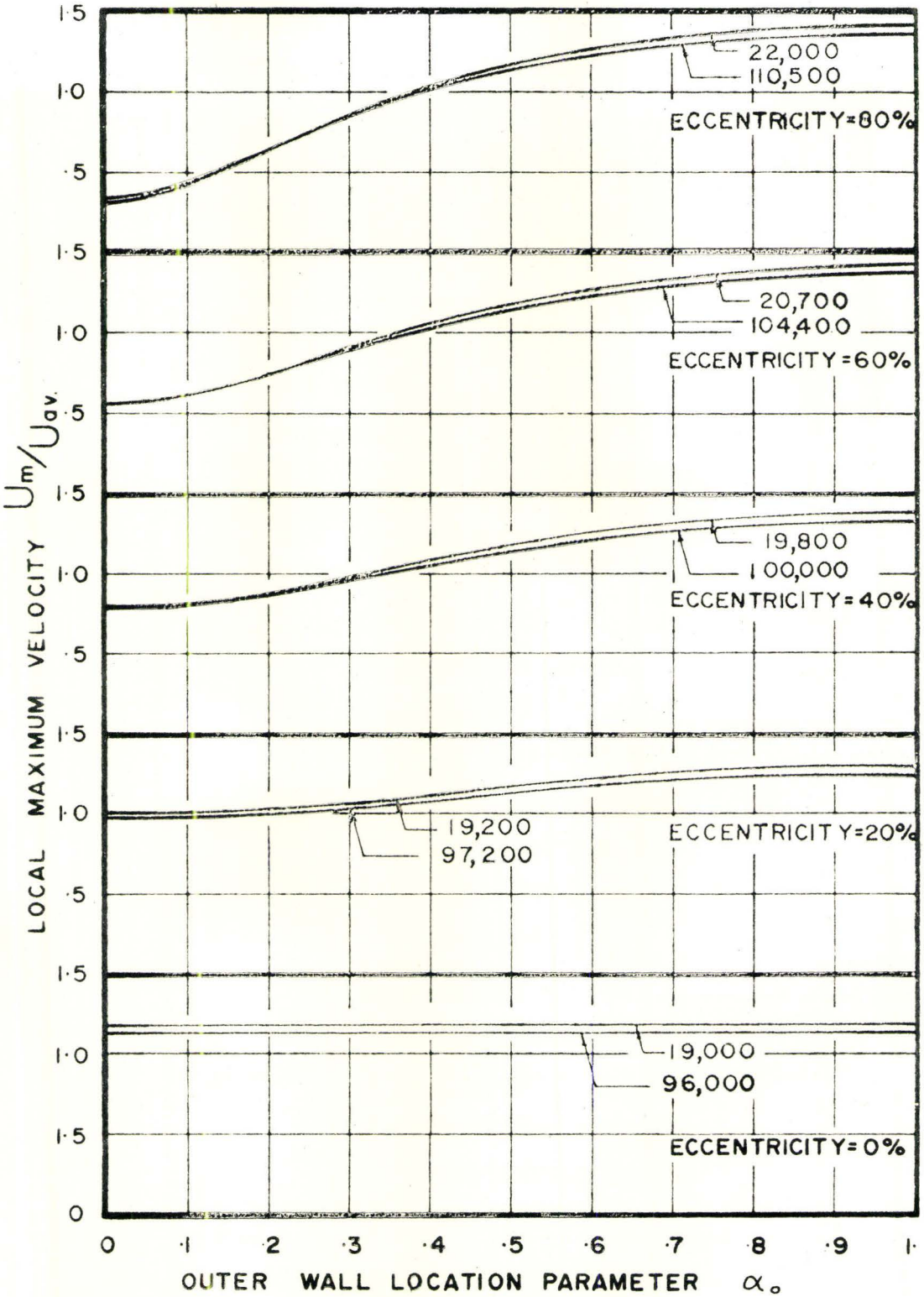


MAXIMUM VELOCITY DISTRIBUTION FOR VARIOUS ECCENTRICITIES

FIGURE 7

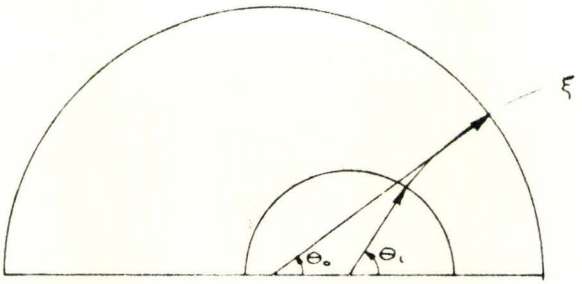


$\alpha_i = \frac{\theta_i}{\pi}$ $\alpha_o = \frac{\theta_o}{\pi}$

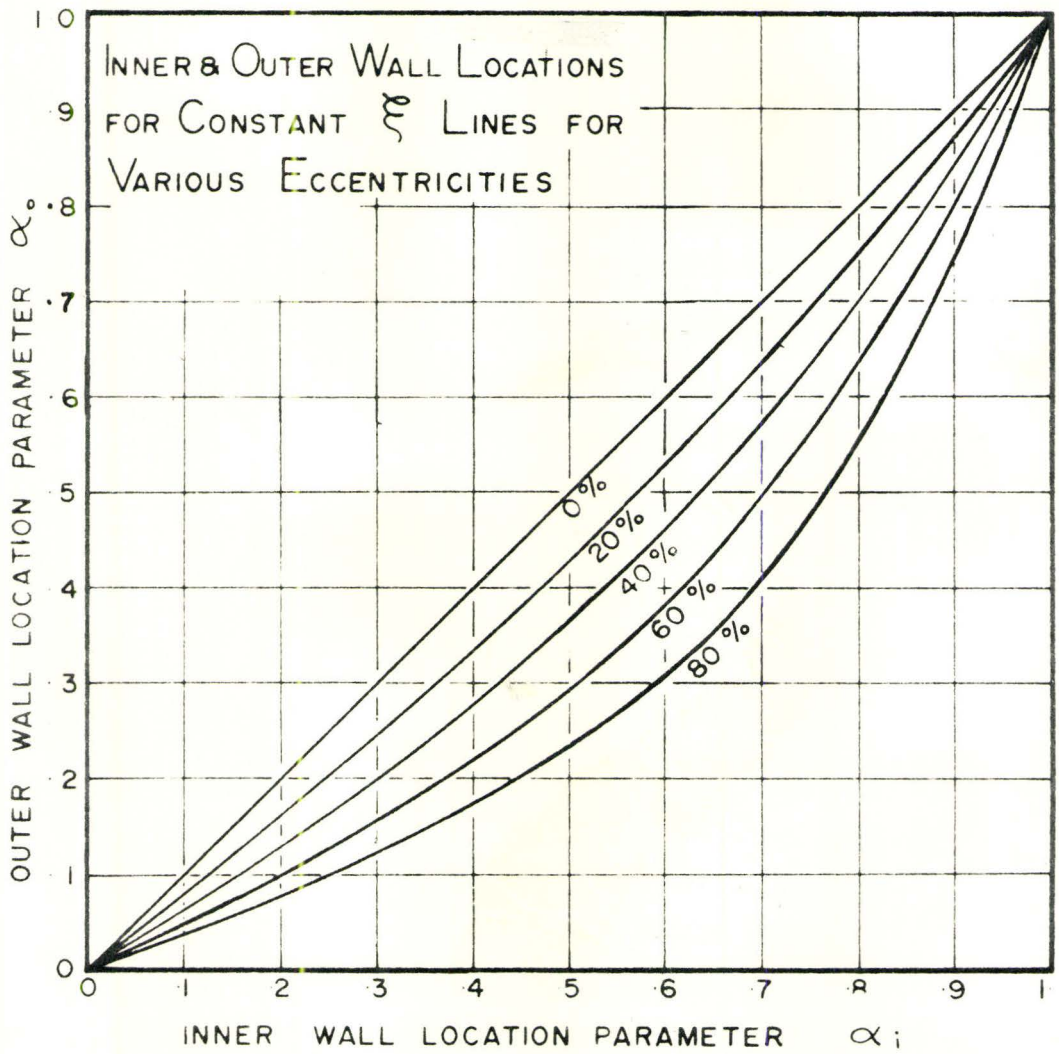

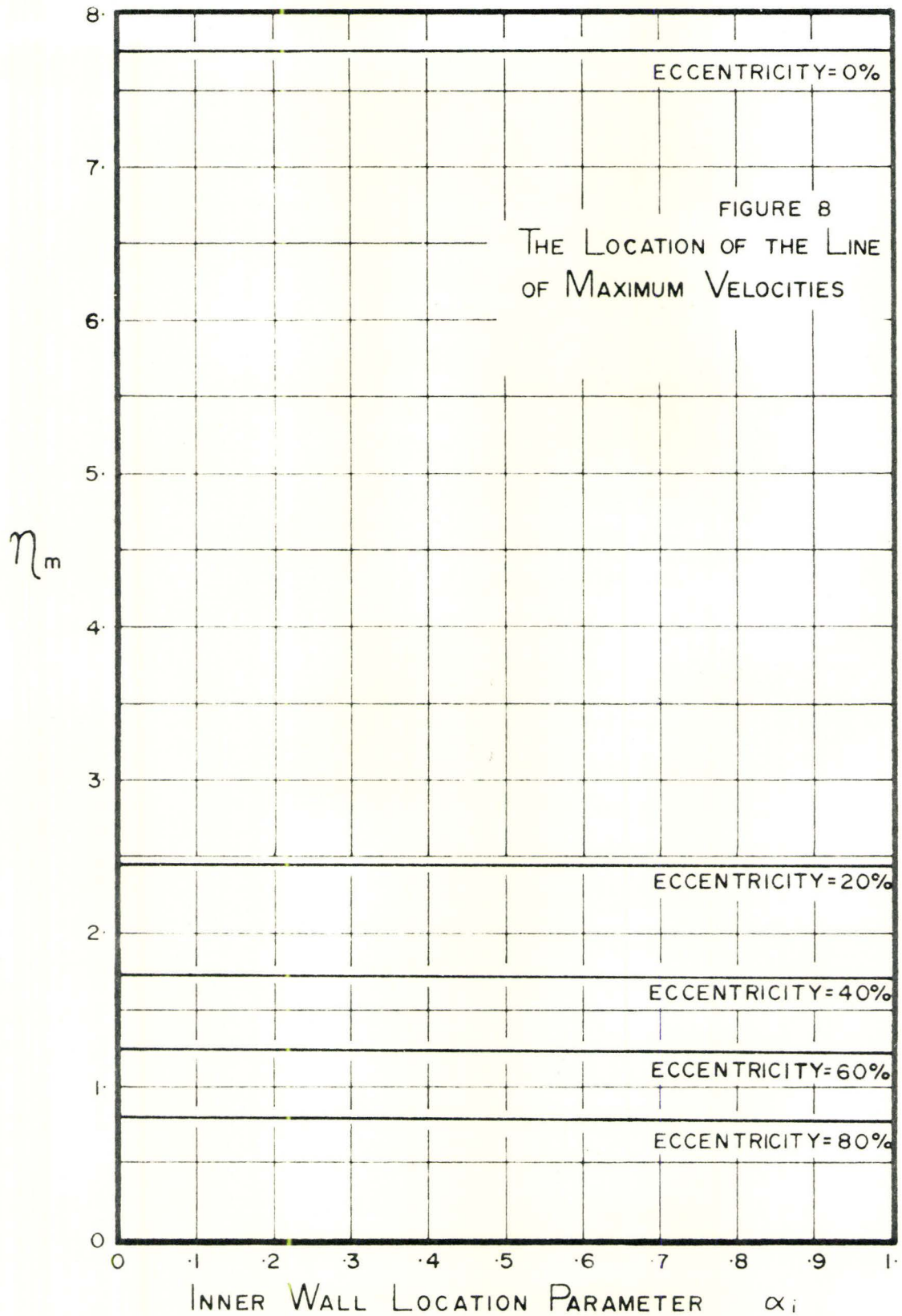


FIGURE 8
THE LOCATION OF THE LINE OF MAXIMUM VELOCITIES

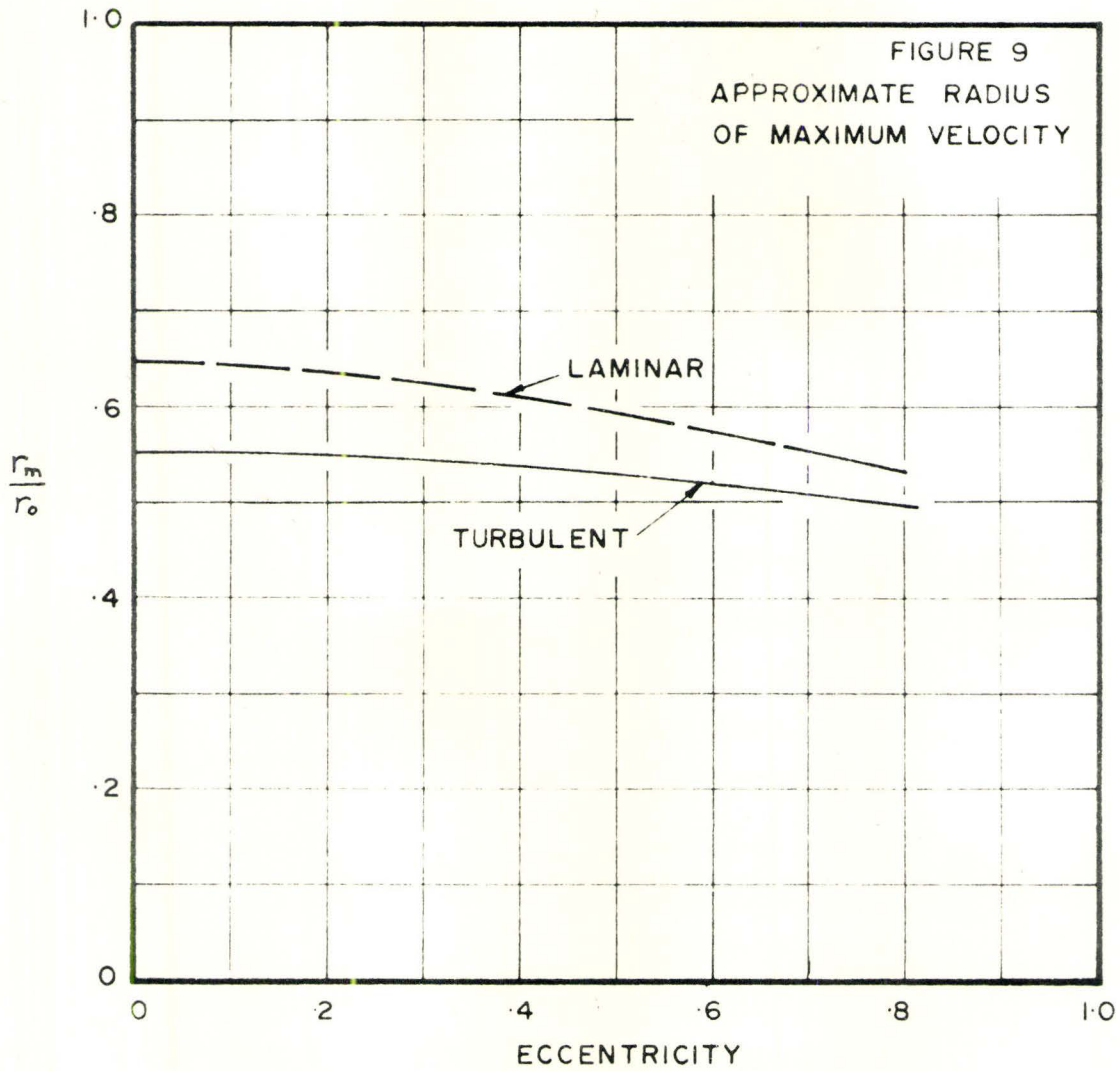
FIGURE 9
APPROXIMATE RADIUS
OF MAXIMUM VELOCITY
LAMINAR
TURBULENT
1·0
·8
·6
·4
·2
0
0
·2
·4
·6
·8
1·0
ECCENTRICITY
r_m / r_o

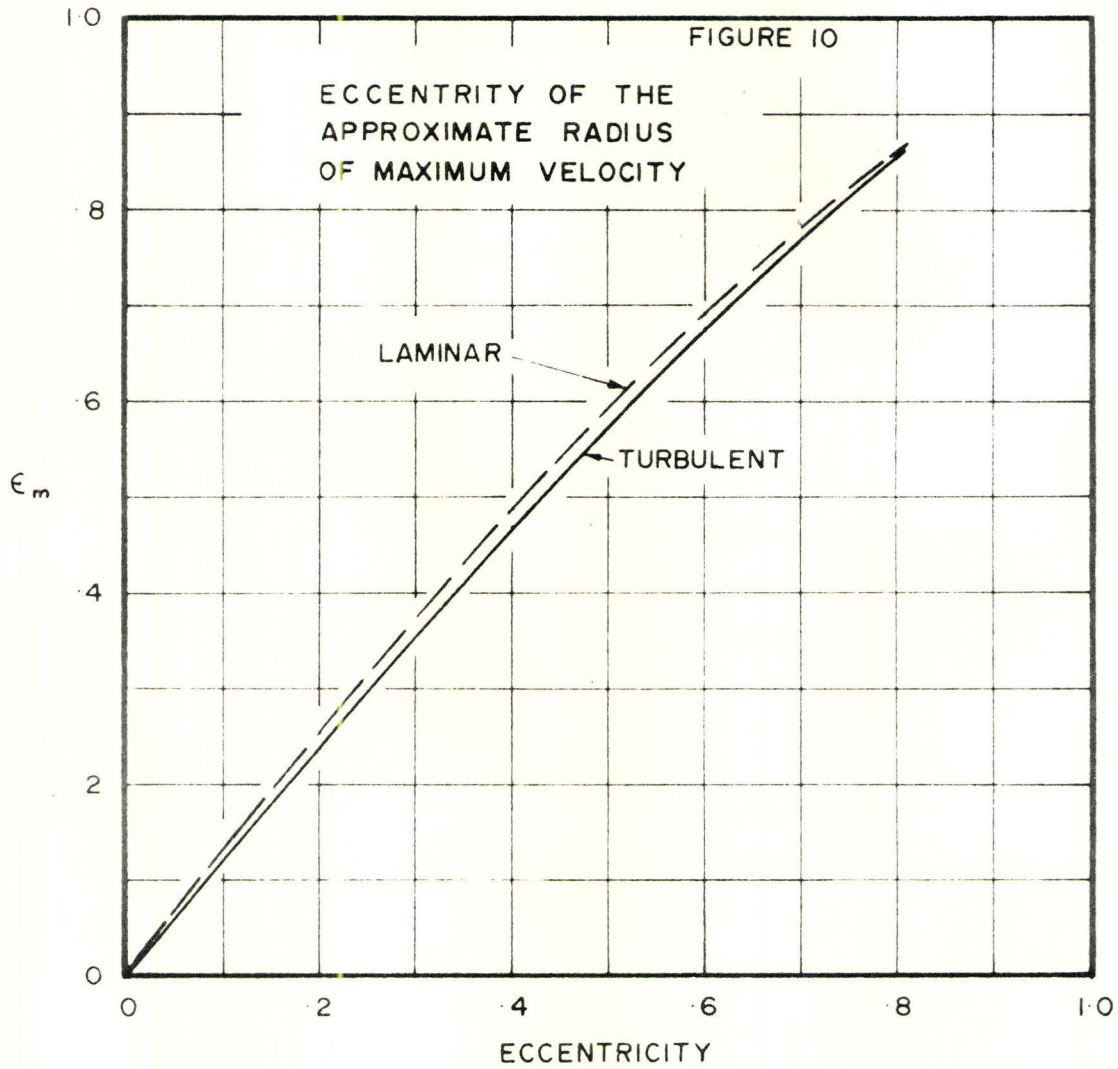
FIGURE 10
ECCENTRITY OF THE
APPROXIMATE RADIUS
OF MAXIMUM VELOCITY
LAMINAR
TURBULENT
$\epsilon_m$
1·0
·8
·6
·4
2
0
0
·2
·4
·6
·8
1·0
ECCENTRICITY

and are compared with Heyda's laminar approximation of equation 5. As the boundaries become more eccentric, the line of maximum velocities shifts towards the inner wall in both cases; however, the turbulent radius is smaller than that of laminar flow in the range considered. This prediction is in keeping with the concentric case which will be discussed separately after the wall friction effects have been presented.

The variations of the inner and outer wall local shear stresses made dimensionless with respect to the local maximum velocities (by dividing by $1/2\ \rho\ U_m^2$) are shown in Figures 11 and 12 for various Reynolds numbers. These friction coefficients are, of course, constant around the walls in the concentric case but are dependent on Reynolds number as shown in Figure 13.

Figure 14 compares the Moody friction factor-Reynolds number relationship for different eccentricities. The decrease in friction factor and thus, of pressure gradient, predicted for increased eccentricity at constant Reynolds number is explained qualitatively by the previously mentioned factor of the large volumetric flow rate in the wide portion of the annulus. As the eccentricity is increased, inspection of Figures 11, 12 and 13 suggests

FIGURE 11

# SHEAR STRESS VARIATION AT THE INNER WALL

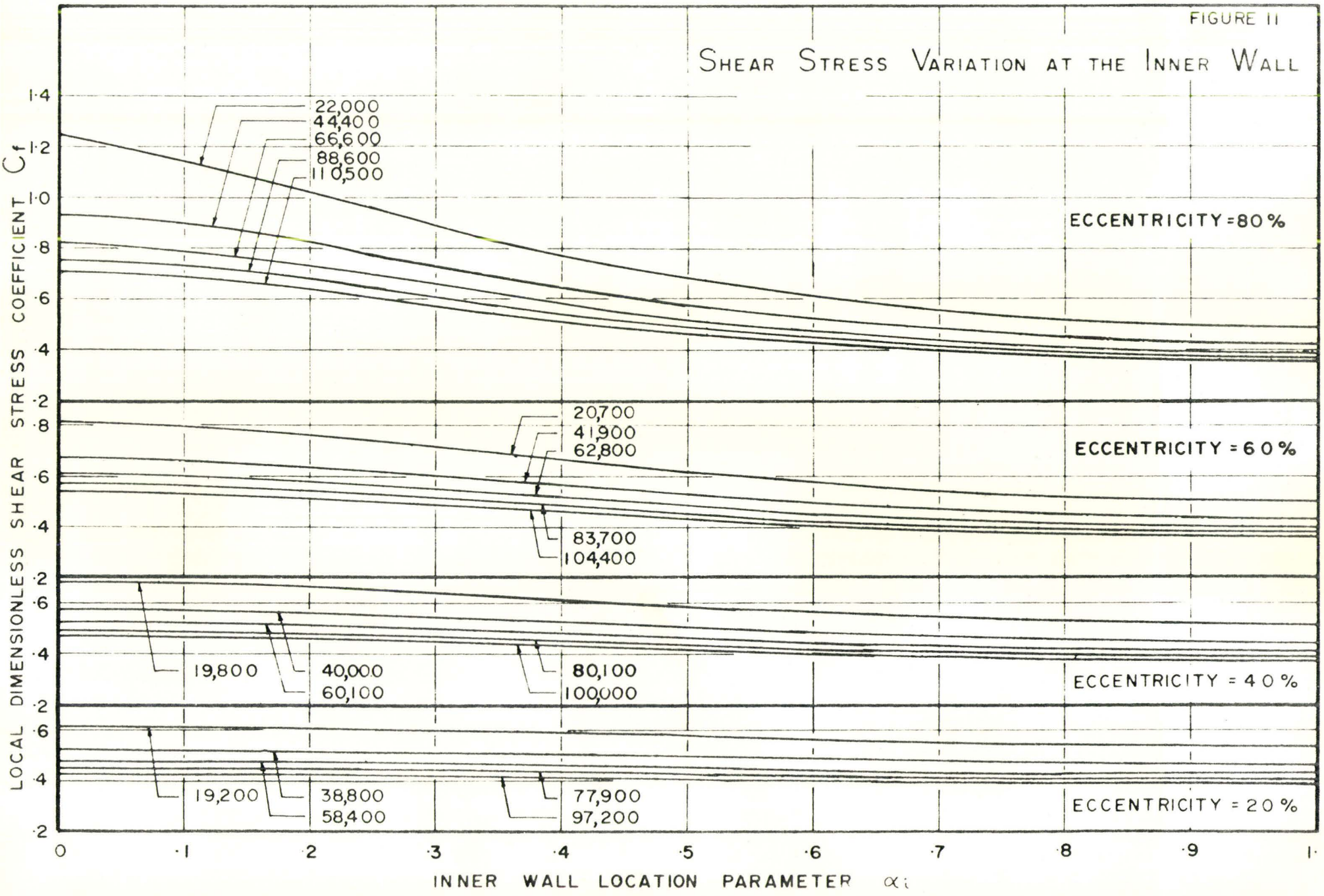

FIGURE 12

# SHEAR STRESS VARIATION AT THE OUTER WALL

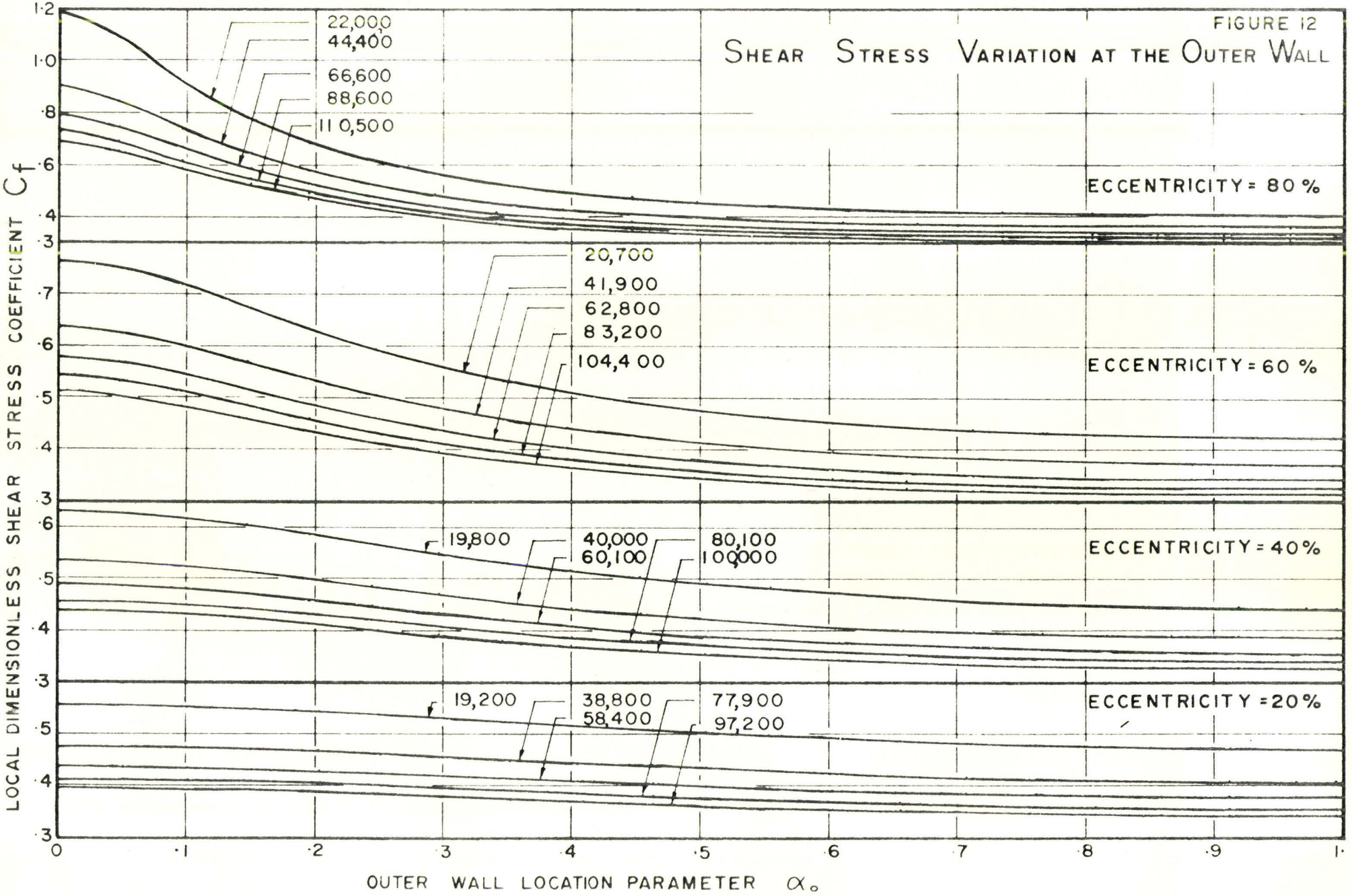

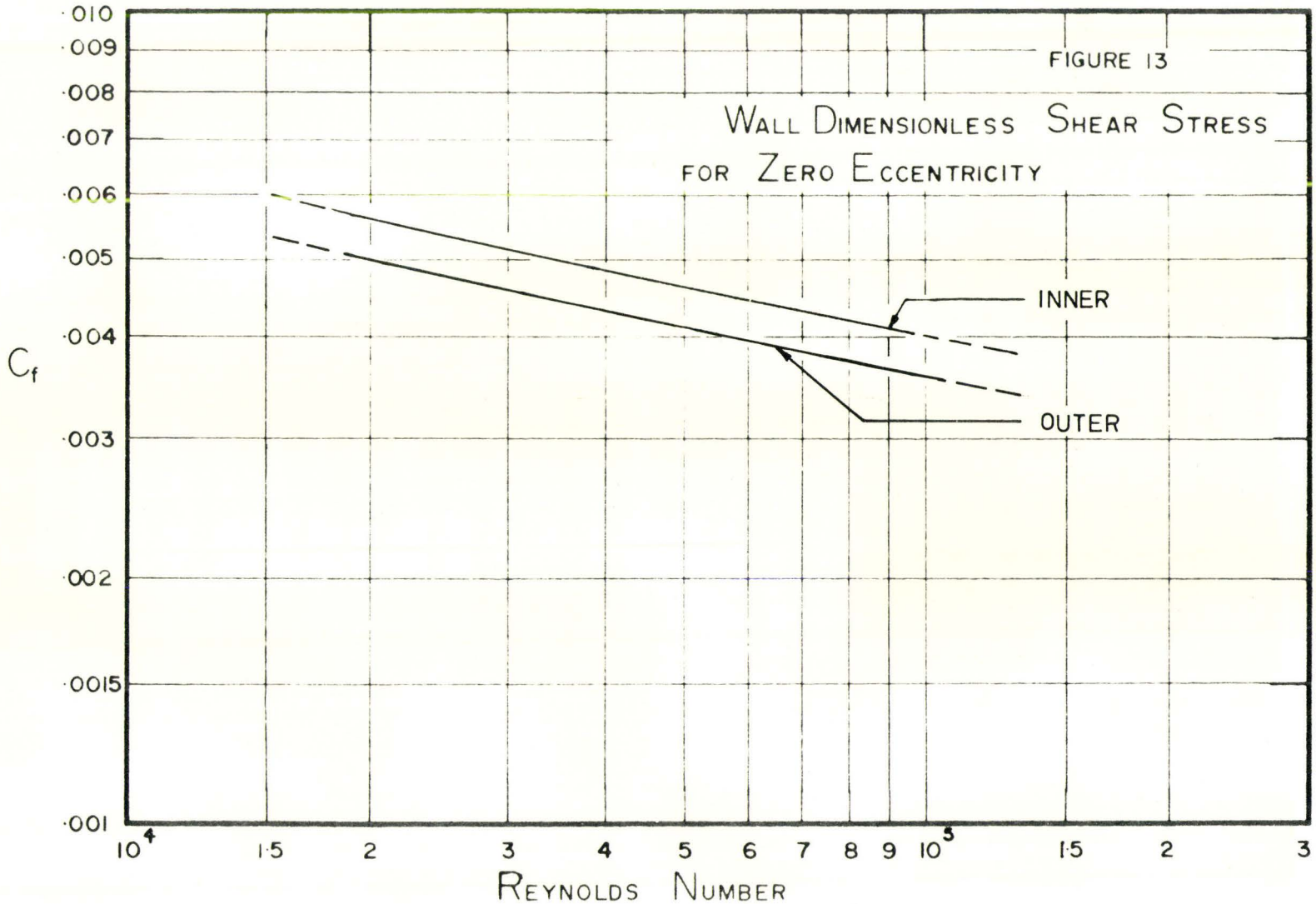
FIGURE 13
WALL DIMENSIONLESS SHEAR STRESS
FOR ZERO ECCENTRICITY
INNER
OUTER
$C_f$
·010
·009
·008
·007
·006
·005
·004
·003
·002
·0015
·001
$10^4$
1·5
2
3
4
5
6
7
8
9
$10^5$
1·5
2
3
REYNOLDS NUMBER

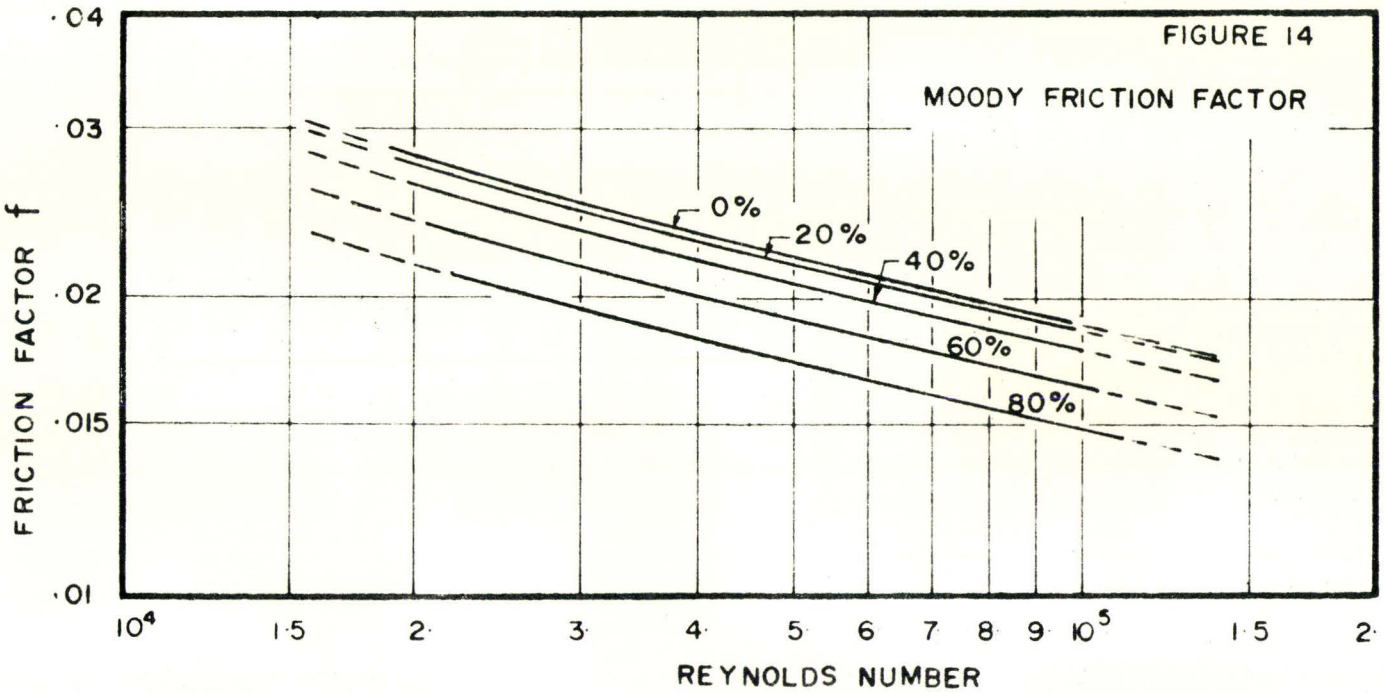
FIGURE 14
MOODY FRICTION FACTOR
FRICTION FACTOR f
·04
·03
·02
·015
·01
0%
20%
40%
60%
80%
10⁴
1·5
2·
3·
4·
5·
6
7
8
9
10⁵
1·5
2·
REYNOLDS NUMBER

that the average value of the dimensionless wall shear stresses is decreased for approximately equal Reynolds numbers with the overall effect of lowering the friction factors.

A widely used application of the annular geometry is the concentric case. This has been investigated extensively by many experimenters and some of their results will be used as a partial test of the foregoing analysis. The friction factors obtained by Brighton and Jones are compared with the predicted variation in Figure 15 for a Reynolds number range from 10,000 to about 400,000. It is seen that the present analysis fits the data somewhat better than the curve for a smooth pipe of the same hydraulic diameter for Reynolds numbers above 40,000. Below this point the present curve lies above the experimental data. Brighton and Jones' data indicates that no significant effect of radius ratio on friction factor exists, and a run of the programme at a radius ratio of 1/2.0 partially confirmed this for the present solution.

Another test of the general validity is obtained by comparing the dimensionless radius of maximum velocity - radius ratio curve with the data of Brighton and Jones, and Ivey in Figure 16. As mentioned in Section 2, they found that these locations were independent

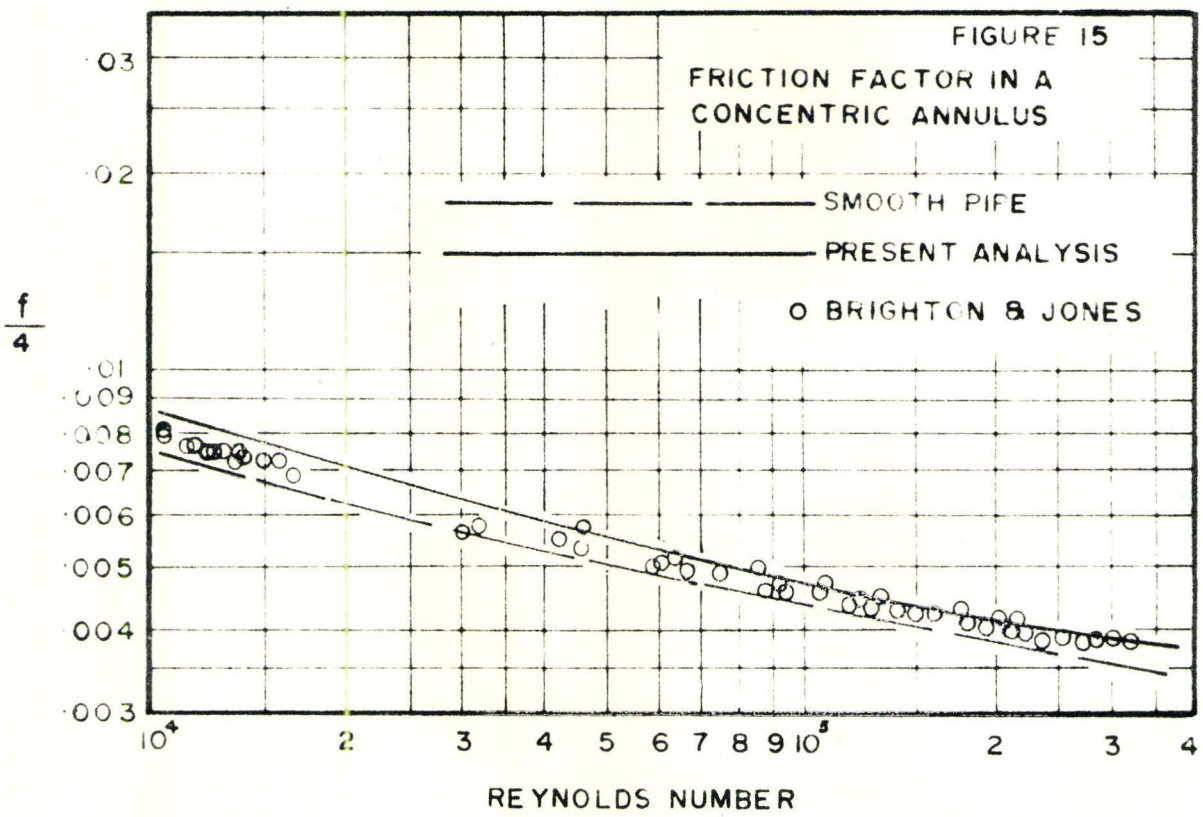
FIGURE 15
FRICTION FACTOR IN A CONCENTRIC ANNULUS
SMOOTH PIPE
PRESENT ANALYSIS
O BRIGHTON & JONES
f/4
.03
.02
.01
.009
.008
.007
.006
.005
.004
.003
10^4
2
3
4
5
6
7
8
9
10^5
2
3
4
REYNOLDS NUMBER

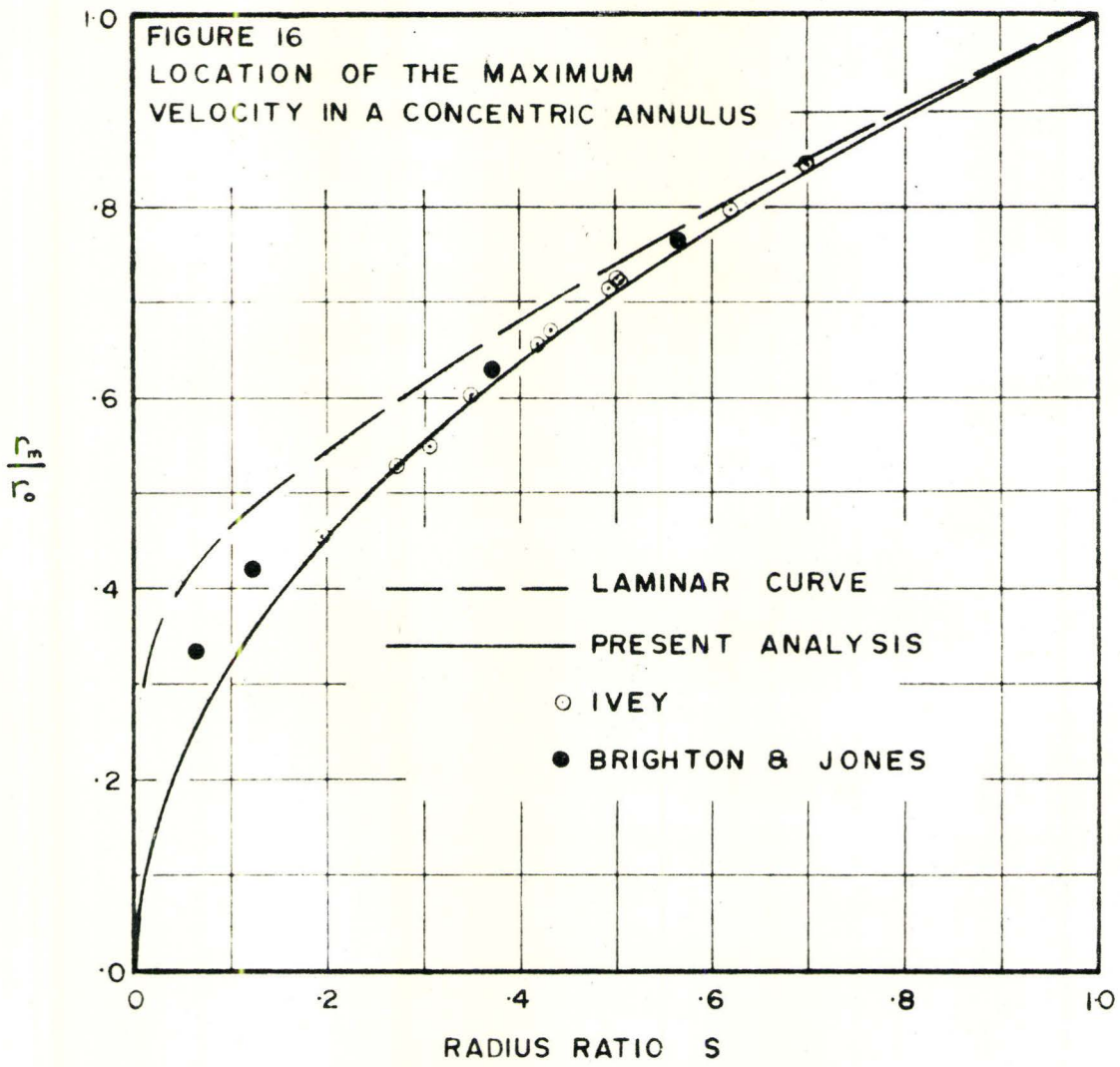
FIGURE 16
LOCATION OF THE MAXIMUM
VELOCITY IN A CONCENTRIC ANNULUS
1·0
·8
·6
·4
·2
·0
0
·2
·4
·6
·8
1·0
$r_o/r$
RADIUS RATIO S
LAMINAR CURVE
PRESENT ANALYSIS
IVEY
BRIGHTON & JONES

of Reynolds number and hydraulic diameter. This fact was confirmed by developing a special programme, described in Section 7.3, and running it for Reynolds numbers of approximately 50,000 and 100,000, and an inner radius of .25 inches and .50 inches with no significant variations being noted. Figure 16 shows that good agreement was obtained with the results for radius ratios greater than about .2. The curve obtained for this analysis lies below the laminar solution for all radius ratios.

## 6. CONCLUSIONS

Velocity fields in both concentric and eccentric annuli have been predicted for fully developed turbulent flow. In the region of the line of maximum velocities the assumed velocity distribution produced an unreasonable mapping of the constant velocity lines. The solution also located the lines of maximum velocities which were found to be independent of Reynolds number and nearer the inner wall than for the laminar solution. In the concentric case the analysis agreed satisfactorily with experimental data above a radius ratio of 0.2.

Both the local wall shear stress variations and the average friction factors were predicted to be dependent on Reynolds number and eccentricity. The concentric friction factors were in good agreement with experimental data.

## 7. APPENDIX

### 7.1 GEOMETRY OF AN ECCENTRIC ANNULUS

The orthogonal coordinate system consistent with the boundaries of an eccentric annulus is described by Heyda. It is given by the complex potential of a source and sink of equal unit strength located at $Z = c$ and $Z = -c$ respectively on the complex x-y plane.

Such a potential is given by

$$W = \ln\left(\frac{Z - c}{Z + c}\right) \quad . \tag{A1}$$

Noting in Figure A1 that $Z$ may be written as

$$Z = -c + r_2 e^{i\theta_2} \quad , \tag{A2}$$

and

$$Z = c + r_1 e^{i\theta_1} \quad , \tag{A3}$$

equation A1 becomes

$$W = \ln \frac{r_1}{r_2} + i(\theta_1 - \theta_2) \quad . \tag{A4}$$

However, points in the W plane may be described by

$$W = \eta + i\xi \quad . \tag{A5}$$

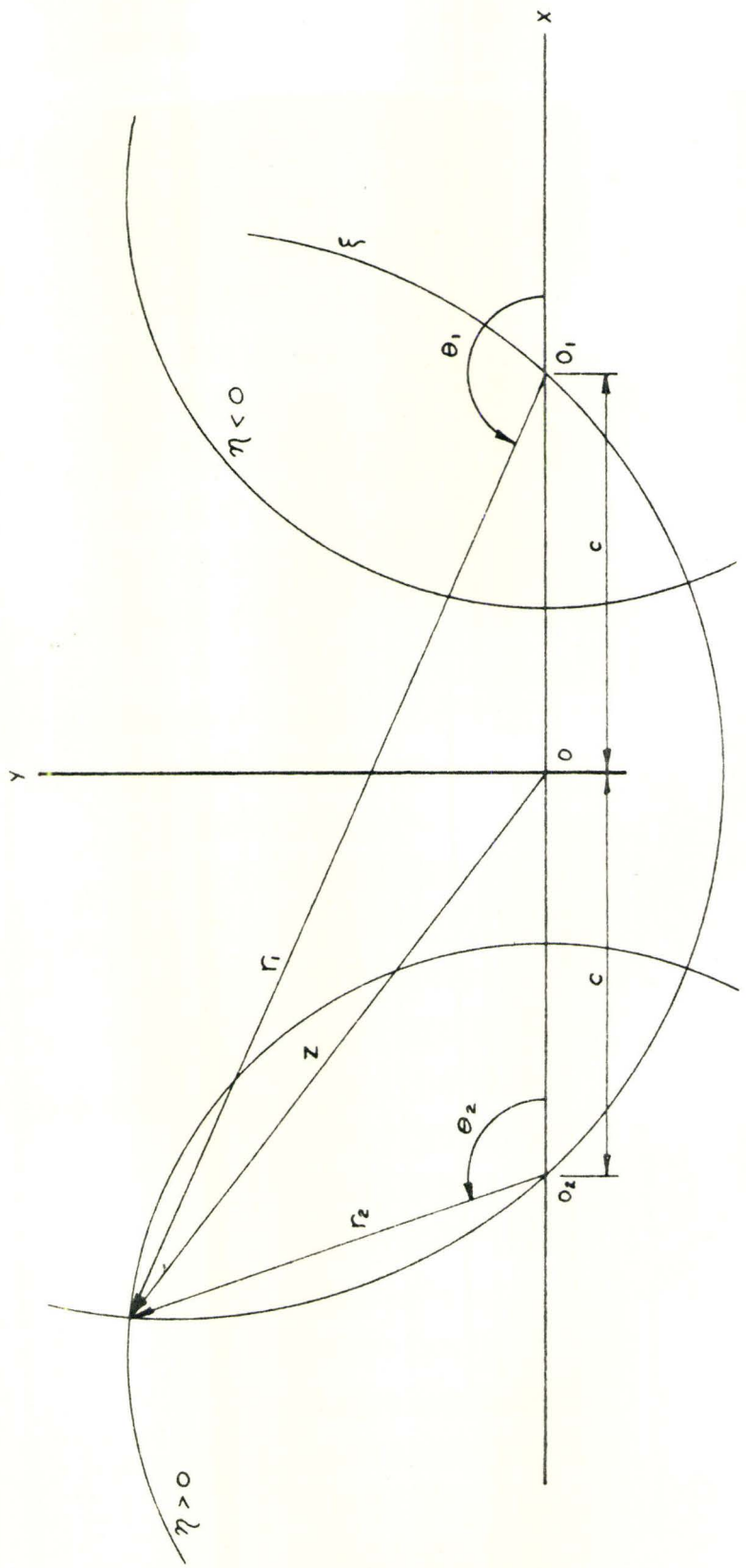


FIGURE A1 COMPLEX Z PLANE

Thus , $\eta = \ln \frac{r_1}{r_2}$ , (A6)

and $\xi = \theta_1 - \theta_2$ . (A7)

In the Z plane $r_1$, $r_2$, $\theta_1$, and $\theta_2$ may be expressed as

$$r_1 = \sqrt{(x-c)^2 + y^2}$$

$$r_2 = \sqrt{(x+c)^2 + y^2}$$

$$\theta_1 = \tan^{-1} \frac{y}{x-c}$$

$$\theta_2 = \tan^{-1} \frac{y}{x+c}$$

Hence $\eta = \ln \sqrt{\frac{(x-c)^2 + y^2}{(x+c)^2 + y^2}}$ , (A8)

and $\xi = \tan^{-1} \frac{y}{x-c} - \tan^{-1} \frac{y}{x+c}$ . (A9)

By writing equation A8 in the exponential form and squaring both sides it can be shown that a constant $\eta$ line in the W plane is transformed into the circle

$$(x + c \coth\eta)^2 + y^2 = c^2 \operatorname{csch}^2 \eta \quad \text{(A10)}$$

in the Z plane. By taking the tangents of both sides of

equation A9 and simplifying, constant $\xi$ lines in the W plane are transformed into circles

$$x^2 + (y - c \cot\xi)^2 = c^2 \cot^2\xi \qquad \text{(A11)}$$

in the Z plane.

In order to describe a particular annulus with an inner radius, $r_i$, an outer radius, $r_o$, and a distance between the centres, $d$, the equations

$$r_i = c \operatorname{csch} \eta_i , \qquad \text{(A12)}$$

$$r_o = c \operatorname{csch} \eta_o , \qquad \text{(A13)}$$

and

$$d = c(\coth \eta_o - \coth \eta_i), \qquad \text{(A14)}$$

which are obtained from equation A10, must be solved for $\eta_i$ and $\eta_o$. In doing this, a radius ratio, $s$, and an eccentricity, $\epsilon$, may be defined as

$$s = \frac{r_i}{r_o} , \qquad \text{(A15)}$$

and

$$\epsilon = \frac{d}{r_o - r_i} . \qquad \text{(A16)}$$

With these definitions, it is possible to show that $\eta_o$ is given by

$$2 \cosh \eta_o = \frac{1+s}{\epsilon} - (1-s)\,\epsilon \quad . \tag{A17}$$

Rewriting equations A12 and A13 gives

$$c = r_o \sinh \eta_o \quad , \tag{A18}$$

and

$$\sinh \eta_i = \frac{c}{r_i} \quad . \tag{A19}$$

Solving equations A10 and A11 for x and y in terms of $\eta$ and $\xi$ yields the transformation equations

$$x = \frac{-c \sinh \eta}{\cosh \eta + \cos \xi} \quad , \tag{A20}$$

and

$$y = \frac{c \sin \xi}{\cosh \eta + \cos \xi} \quad . \tag{A21}$$

The arc length, $dS_\xi$, along a constant $\xi$ line can be shown to be

$$dS_\xi = \frac{-c\, d\eta}{\cosh \eta + \cos \xi} \quad . \tag{A22}$$

Similarly, the arc length, $dS_\eta$ along a constant $\eta$ line is

given by

$$dS_\eta = \frac{c\, d\xi}{\cosh\eta + \cos\xi} \quad . \tag{A23}$$

An element of area, $dA$, is

$$dA = \frac{-\, c^2\, d\eta\, d\xi}{(\cosh\eta + \cos\xi)^2} \quad . \tag{A24}$$

These three equations are difficult to integrate. While equation A24 may, best be integrated numerically, a direct geometrical approach may be used to replace equations A22 and A23.

For example, in Figure A2, the chord length between two points $(\eta_o, \xi)$ and $(\eta_m, \xi)$ on a constant $\xi$ line is

$$L_\xi = \sqrt{(x(\eta_o,\xi) - x(\eta_m,\xi))^2 + (y(\eta_o,\xi) - y(\eta_m,\xi))^2} \quad , \tag{A25}$$

where $x(\eta,\xi)$ and $y(\eta,\xi)$ are given by equations A20 and A21. Thus, the half angle enclosed by the radii from the centre of the circle $\xi$ = a constant to the points $(\eta_o, \xi)$ and $(\eta_m, \xi)$ is

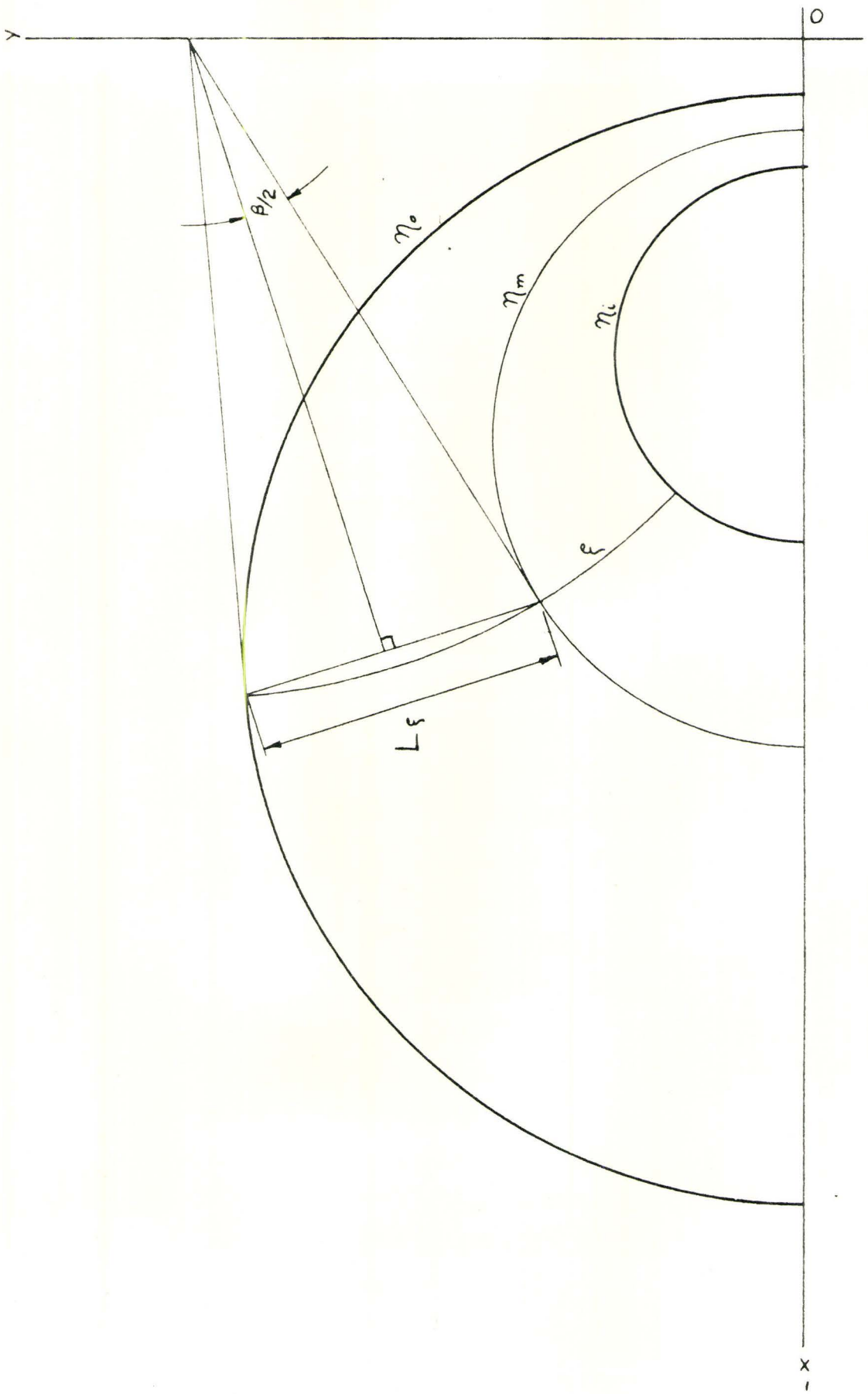


FIGURE A2 ARC LENGTH DETERMINATION

$$\frac{\beta_\xi}{2} = \sin^{-1}\left(\frac{L_\xi}{2c\csc\xi}\right) .$$

The arc length, $S_\xi$, along the constant $\xi$ curve between the two points is

$$S_\xi = 2c \csc\xi \sin^{-1}\left(\frac{L_\xi}{2c\csc\xi}\right),$$

or

$$S_\xi = \frac{2c}{\sin\xi} \sin^{-1}\left(\frac{L_\xi \sin\xi}{2c}\right) . \qquad \text{(A26)}$$

Similarly, the chord length along a constant $\eta$ line between $(\eta, \xi_1)$ and $(\eta, \xi_2)$ is

$$L_\eta = \sqrt{(x(\eta,\xi_1) - x(\eta,\xi_2))^2 + (y(\eta,\xi_1) - y(\eta,\xi_2))^2} . \qquad \text{(A27)}$$

The half angle, $\frac{\beta_\eta}{2}$ is

$$\frac{\beta_\eta}{2} = \sin^{-1}\left(\frac{L_\eta}{2c\ \mathrm{csch}\ \eta}\right) ,$$

and the arc length, $S_\eta$, is

$$S_\eta = \frac{2c}{\sinh \eta} \sin^{-1}\left(\frac{L_\eta \sinh \eta}{2c}\right) . \qquad \text{(A28)}$$

## 7.2 COMPUTER SOLUTION FOR THE VELOCITY FIELDS IN ECCENTRIC ANNULI

By the application of FORTRAN IV language to the equations developed in Section 3, a numerical solution for the velocity fields in eccentric annuli can be obtained. The final form of the solution is included in this section with explanatory remarks on appropriately placed comment cards. These cards in the programme are identified by a letter c in the extreme left hand space. They serve to explain and identify the calculations performed in the immediately following portion of the programme. In addition, a summary of the important FORTRAN symbols and a brief description of the programme are included to clarify the actual solution.

First, the important symbols are tabulated below:

| FORTRAN SYMBOL | DESCRIPTION |
|---|---|
| A(J,IA) | Inner and outer incremental areas, $A_i$ and $A_o$, respectively. |
| AR(J,K) | Intermediate incremental areas for specified value of $\xi$ |

| FORTRAN SYMBOL | DESCRIPTION |
|---|---|
| AWS | Final value is average velocity, $U_{av}$ |
| CF(J,IA) | Inner and outer wall dimensionless shear stress, $C_f$ |
| DISS(J,IA) | Inner and outer wall location parameters, $\alpha_i$ and $\alpha_o$ |
| DPDZ | Pressure gradient, $\frac{dP}{dz}$ |
| EPS(I) | $\xi$ coordinate |
| EPSM(I) | $\xi_1$ value identified with $\xi$ |
| EPSP(I) | $\xi_2$ values identified with $\xi$ |
| ETA(1) | $\eta$ coordinate of inner wall, $\eta_i$ |
| ETA(2) | $\eta$ coordinate of outer wall, $\eta_o$ |
| ETA(3) | $\eta$ coordinate of line of maximum velocities for laminar flow, $\eta_{ml}$ |
| ETAS | $\eta$ coordinate of line of maximum velocities for turbulent flow, $\eta_m$ |
| EXC | Eccentricity of the annular geometry, $\epsilon$ |

| FORTRAN SYMBOL | DESCRIPTION |
|---|---|
| F | Moody friction factor, $f$ |
| G | Gravitational constant = 32.174, $g_c$ |
| I | Index used in connection with increasing values of $\xi$ |
| IA | Index used to describe values of $\xi$ at which the solution is applied |
| J | Index used to reference inner or outer section. For the inner section J = 1, for the outer J = 2 |
| K | Index used to describe values of $\eta$ along a constant $\xi$ line |
| RA(1) | Subscripted form of radius of inner wall, $r_i$ |
| RA(2) | Subscripted form of radius of outer wall, $r_o$ |
| RADIUS (IA) | Radius of constant $\xi$ line specified by IA |
| RE | Reynolds Number of calculated velocity field, Re |
| REY(IN) | Approximate Reynolds Number at input |
| RHO | Fluid density, $\rho$ |
| RI | Inner wall radius, $r_i$ |
| RO | Outer wall radius, $r_o$ |

| FORTRAN SYMBOL | DESCRIPTION |
|---|---|
| S(J,I) | Incremental lengths identified with a value of $\xi$ along the inner and outer walls, $S_\eta$ |
| SUM(J) | Summation of $S(J,I)$'s from $\xi = 0$ line |
| VIS | Kinematic viscosity, $\nu$ |
| VV(J,IA,K) | Velocity distribution throughout the flow field |
| WW(J,IA) | Volumetric discharges through areas identified by values of $\xi$ at which the solution was applied |
| WWW(I) | Volumetric discharges for each value of $\xi$ identified by EPS(I) |
| Y(J,K) | Distance of point $(\eta, \xi)$ from the wall in question along constant $\xi$ line, $Y$ |
| YY(J,IA,K) | $\eta$ coordinate determined by integration method along constant $\xi$ lines. |

The input data for the programme consists of the inner and outer wall radii, the eccentricity, the fluid density and kinematic viscosity, the gravitational constant and the approximate Reynolds Numbers. The first step in the programme is to evaluate the $\eta$ coordinates of the inner and outer walls and the approximate line of maximum velocities for laminar flow. This value is used later as a first estimate of $\eta_m$ for turbulent flow.

Since the solution of the velocity field results from a known pressure gradient, the actual Reynolds Number is unknown until the calculations are completed. However, control over the final Reynolds Number is obtained by using a linear approximation to the Moody diagram in conjunction with the input Reynolds Number. Thus, a realistic pressure gradient is determined for use in the succeeding calculations.

As the solution depends on the use of finite incremental areas, a problem existed in determining a suitable increment of the $\xi$ coordinate to be used in the numerical calculations. Some preliminary work evaluated the total flow area by means of equations 8 and 9 using fourteen point

Gaussian integrations in each coordinate direction with $\xi_1$ and $\xi_2$ differing successively by $\pi/180$ radians. The values so obtained for the five configurations agreed to at least the fifth significant figure with the area calculated by $A = \pi(r_o^2 - r_i^2)$. Thus, the increments were chosen to be $\pi/180$ for the computer programme.

For convenience, the programme was developed to consider successive values of $\xi$ equal to $\pi/360$, $3\pi/360$, ... $359\pi/360$, with corresponding values of $\xi_1$ equal to $0$, $\pi/180$, .. .. $179\pi/180$, and $\xi_2$ equal to $\pi/180$, $2\pi/180$, .... $\pi$. The incremental arc lengths around the inner and outer walls between $\xi_1$ and $\xi_2$ are evaluated for each value of $\xi$. For the first and last values of $\xi$ and about twenty intermediate values spaced around the outer wall, the computer proceeds to determine the correct value of $\eta_m$.

This is done by evaluating the two incremental areas and wall shear stresses in order to obtain two values of velocity at each estimated value of $\eta_m$. These two velocities are matched to within $0.1\%$ by shifting the value of $\eta_m$ in a trial and error manner.

The programming method is such that the values of velocity along constant $\xi$ lines are calculated at the values of $\eta$ determined by the Gaussian integration

subroutine. Similarly, numerical representations of small sections of the incremental areas are identified with the same values of $\eta$ . Thus, by using the same integration subroutine, the volumetric discharges through the incremental areas are readily calculated.

This procedure is repeated for the values of $\xi$ mentioned previously. Then, the total discharge is obtained by a five point interpolation for the intermediate values and summation over the entire area. After the correct values of the Reynolds Number and friction factor are calculated, the inner and outer radii, the eccentricity, the Reynolds Number, the Moody friction factor and the average velocity are printed out.

At this stage in the calculations, the problem is essentially solved. The velocity distribution, the wall shear stress and the $\eta_m$ coordinate value are known for conveniently spaced constant $\xi$ lines. However, the data may be put into a more concise form for graphical presentation.

The velocity distribution is made dimensionless with respect to the average velocity. By interpolation to find the $(\eta, \xi)$ coordinates of specified values of $U/U_{av}$,

the ( $x$, $y$ ) coordinates of points on representative constant velocity lines are determined. This permits the use of an on line plotting subroutine to produce a constant velocity map of the flow field. (This mapping is not desired in all cases and can be prevented, with a noticeable saving of running time, by setting the input value of VERS equal to zero).

Determining the inner and outer wall location parameters corresponding to the values of $\xi$ which were used and making the wall shear stresses dimensionless with respect to the local maximum velocities complete the computer calculations. The output data consists of the values of $\xi$ at which the solution was obtained, the $\eta_m$ distribution, the variation of the ratio $U_m/U_{av}$, the inner and outer wall location parameters, and the dimensionless wall shear stress coefficients.

This programme was run for a radius ratio of 1/3.5, and for eccentricities of .001, .20, .40, .60, .80. (The digital solution produces a floating point overflow if the eccentricity is set equal to zero). Input Reynolds Numbers from 20,000 to 100,000 in steps of 20,000 were used for each configuration to produce the results discussed in Section 5.

```
$IBFTC EAVP3
      DIMENSION ETA(3),RA(2),WWW(180),S(2,180),A(2,25),T(2,25),Q(2),SL(2
     1),B(2),WW(2,25),X(25),YYY(25),SUM(2),COSH(2),SINH(2),XSM(2),YSM(2)
     2,XSP(2),YSP(2),VELO(20),XXL(600),YYL(600),NN(25),V(2,25) , XA(2),
     3DISS(2,25),CF(2,25 ,REY(5)
      COMMON I,J,K,EPSM(180),EPS(180),EPSP(180),XS(2,25),YS(2,25),RADIUS
     1(25),YY(2,25,15),AR(2,15),CCOSH,PP(2,15),VV(2,25,15),Y(2,15),C,IA
C  READ IN DATA
      READ(5,1)RI,RO,EXC
    1 FORMAT(3F6.3)
      READ(5,2)RHO,G,VIS
    2 FORMAT(3F10.7)
      READ(5,500)(VELO(II),II=1,12 )
  500 FORMAT(12F4.2)
      READ(5,501)(REY(IN),IN=1,5),VERS
  501 FORMAT(6F10.0)
C  CALCULATE CONSTANTS OF ANNULAR GEOMETRY
      PI=4.*ATAN(1.0)
      DUM=(1.+RI/RO)/EXC+(1.-RI/RO)*EXC
      ETA(2)=ALOG(DUM/2.+SQRT(DUM*DUM/4.-1.))
      C=  (EXP(ETA(2))-EXP(-ETA(2)))/2.    *RO
      ETA(1)=ALOG(C/RI+SQRT(C*C/RI/RI+1.))
      DUM=.5*(SQRT((1.-TANH(ETA(1)))*(1.+TANH(ETA(2))))+SQRT((1.+TANH(ET
     1A(1)))*(1.-TANH(ETA(2)))))
```

```
      ETA(3)=ALOG(1./DUM+SQRT(1./DUM/DUM-1.))
      DUM=.5*PI/180.
      RA(1)=RI
      RA(2)=RO
      OUTER=PI*RO/21.
      EXTERNAL AREA
      EXTERNAL VOL
      EXTERNAL VEL
      DO 48 IN=1,5
      DO 33 J=1,2
      CENT=-C/TANH(ETA(J))
      XXL(J)=CENT
   33 YYL(J)=0.
C  DETERMINE F AND DPDZ FOR APPROXIMATE RE
      RE=REY(IN)
      F=EXP(-0.2338*ALOG(RE)-1.34)
      DPDZ=F*(RE*6.*VIS/(RO-RI))**2/((RO-RI)*G/3.)*RHO
      WRITE(7,700)RI,RO,EXC,RE,DPDZ,ETA(1),ETA(2)
  700 FORMAT(3F6.3,F10.0,3E15.8)
      SUM(1)=0.
      SUM(2)=0.
      KK=3
      IA=1
      DO 4 I=1,180
      D=I
```

```
C  GENERATE VALUES OF EPS,EPSM,AND,EPSP
      EPSP(I)=D*PI/180.
      EPS(I)=EPSP(I)-DUM
      EPSM(I)=EPS(I)-DUM
      DO 3 J=1,2
      IF(I.GT.1) GO TO 6
      DUM1=EXP(-ETA(J))
      COSH(J)=(EXP(ETA(J))+DUM1)/2.
      SINH(J)=COSH(J)-DUM1
      XSM(J)=-C*SINH(J)/(COSH(J)+COS(EPSM(I)))
      YSM(J)=-XSM(J)/SINH(J)*SIN(EPSM(I))
      GO TO 23
    6 XSM(J)=XSP(J)
      YSM(J)=YSP(J)
   23 DUP=COSH(J)+COS(EPSP(I))
      XSP(J)=-C*SINH(J)/DUP
      YSP(J)=C*SIN(EPSP(I))/DUP
C  CALCULATE VALUE OF INCREMENTAL LENGTH ALONG THE WALLS
      S(J,I)=RA(J)*ARSIN(SQRT((XSP(J)-XSM(J))**2+(YSP(J)-YSM(J))**2)/2./
     1RA(J))*2.
    3 SUM(J)=S(J,I)+SUM(J)
C  BEGIN VELOCITY DISTRIBUTION CALCULATIONS FOR SUITABLE VALUES OF EPS
      IF(I.EQ.1) GO TO 40
      IF(I.EQ.180)GO TO 40
      IF(SUM(2).LT.OUTER)GO TO 4
```

```
   40 SUM(2)=0.
      RADIUS(IA)=C/SIN(EPS(I))
      NN(IA)=I
      IF(I.EQ.1) ETAS=ETA(3)
      L=1
C  START OF ITERATION LOOP FOR LINE OF MAXIMUM VELOCITY
    5 DO 63 JJ=1,2
      J=JJ
      K=1
      IF(L.GT.1) GO TO 21
      XS(J,IA)=-C*SINH(J)/(COSH(J)+COS(EPS(I)))
      YS(J,IA)=-XS(J,IA)/SINH(J)*SIN(EPS(I))
C  INCREMENTAL AREA CALCULATION
   21 A(J,IA)=C*C*GINTZ4(AREA,ETA(J),ETAS)
      DUM1=EXP(-ETAS)
      CCOSH=(EXP(ETAS)+DUM1)/2.
      SSINH=CCOSH-DUM1
      XX=-C*SSINH/(CCOSH+COS(EPS(I)))
      YX=-XX/SSINH*SIN(EPS(I))
C  DISTANCE OF LINE OF MAXIMUM VELOCITY FROM THE WALLS ALONG CONSTANT
C  EPS LINE
      Y(J,15)=RADIUS(IA)*ARSIN(SQRT((XX-XS(J,IA))**2+(YX-YS(J,IA))**2)/2
     1./RADIUS(IA))*2.
C  SHEAR STRESS AT WALLS
      T(J,IA)=DPDZ*A(J,IA)/S(J,I)/12.
```

```
      SV=SQRT(T(J,IA)/RHO*G)
      PPP=0.
      VL=0.
C  VELOCITY PROFILES ALONG CONSTANT EPS LINE
      DO 7 K=1,15
      PP(J,K)=Y(J,K)/12.*SV/VIS
      VV(J,IA,K)=SV*GINT24(VEL,PPP,PP(J,K))+VL
      PPP=PP(J,K)
    7 VL=VV(J,IA,K)
   63 V(J,IA)=VV(J,IA,15)
C  CHECK OF MATCHING AT LINE OF MAXIMUM VELOCITY
      IF(ABS(1.-V(1,IA)/V(2,IA)).LT..0001) GO TO 9
      IF(L.GT.1) GO TO 8
C  FIRST PREDICTION OF ETAS
      Q(1)=V(1,IA)
      Q(2)=V(2,IA)
      E=ETAS
      ETAS=ETAS+.03
      L=2
      GO TO 5
C SECOND AND SUBSEQUENT PREDICTION OF ETAS
    8 DO 12 J=1,2
      SL(J)=(V(J,IA)-Q(J))/(ETAS-E)
   12 B(J)=V(J,IA)-SL(J)*ETAS
      ETAS=(B(2)-B(1))/(SL(1)-SL(2))
```

```
      L=L+1
      IF(L.GT.20)STOP
      GO TO 5
C  CALCULATE VOLUMETRIC DISCHARGE FOR INCREMENTAL AREAS
    9 DO 14 JJ=1,2
      J=JJ
      K=1
      WW(J,IA)=C*C*GINTZ4(VOL,ETA(J),ETAS)
      IF(WW(J,IA).LT.0.0) WW(J,IA)=-WW(J,IA)
      YY(J,IA,15)=ETAS
   14 CONTINUE
      IA=IA+1
    4 CONTINUE
      IA=IA-1
      WRITE(7)(NN(I),YY(1,I,15),I=1,IA)
      K=3
      AWS=0.
C  INTERPOLATION OF VOLUMETRIC DISCHARGE IN INTERMEDIATE SECTIONS
      DO 31 I=1,IA
   41 X(K)=WW(1,I)+WW(2,I)
      NNN=NN(I)
      YYY(K)=EPS(NNN)
      M=K
      K=K+1
   31 CONTINUE
```

```
      X(1)=X(4)
      X(2)=X(3)
      YYY(1)=-YYY(4)
      YYY(2)=-YYY(3)
      X(K)=X(M)
      YYY(K)=PI/180.*180.5
      DO 32 I=1,180
      XX=EPS(I)
      L=0
      N=5
      DO 35 K=1,M
      IF(XX.EQ.YYY(K)) GO TO 36
   35 IF(XX.GT.YYY(K).AND.XX.LT.YYY(K+1)) L=K-2
      IF(L.LE.0)L=1
      IF(L.GT.M-3) L=M-3
      WWW(I)=POLINT(YYY,X,N,XX,L)
      GO TO 32
   36 WWW(I)=X(K)
C SUMMATION OF VOLUMETRIC DISCHARGE OVER FLOW AREA
   32 AWS=AWS+WWW(I)
C DETERMINE AVERAGE VELOCITY
      AWS=AWS/PI/(RO**2-RI**2)*2.
C  CALCULATE CORRECT F AND RE
      F=DPDZ*(RO-RI)*G/AWS/AWS/RHO/3.
      RE=(RO-RI)*AWS/6./VIS
```

```
      WRITE(6,103)RO,RI,EXC,RE,F,AWS
  103 FORMAT(1H1,///,1H0,13HOUTER RADIUS=,F10.3,10X,13HINNER RADIUS=,F10
     1.3,10X,13HECCENTRICITY=,F10.3,//1H0,16HREYNOLDS NUMBER=,F8.0, 9X,
     216HFRICTION FACTOR=,F8.5, 9X,17HAVERAGE VELOCITY=,F7.3)
      YMAX=XXL(2)+RO
      YMIN=XXL(2)-RO-.25
      XMAX=RO
      XMIN=0.
      WRITE(6,515)
  515 FORMAT(1H0,6H INDEX,4X,2HXI,7X,4HETA*,6X,4HVMAX,6X,6HALPHAI,8X,3HC
     1FI,8X,6HALPHAO,8X,3HCFO)
      DO 43 J=1,2
   43 XA(J)=XXL(J)+RA(J)
      DO 10 I=1,IA
      DO 45 J=1,2
      DO 46 K=1,15
C     MAKE VELOCITY DISTRIBUTION DIMENSIONLESS
   46 VV(J,I,K)=VV(J,I,K)/AWS
C  DETERMINE INNER AND OUTER WALL LOCATION PARAMETERS
      DISS(J,I)=ARSIN(SQRT((XA(J)-XS(J,I))**2+YS(J,I)**2)/2./RA(J))*2./
     1PI
C     MAKE WALL SHEAR STRESSES DIMENSIONLESS
   45 CF(J,I)=T(J,I)/(RHO*V(J,I)**2)*2.*G
      NNN=NN(I)
   10 WRITE(6,502)NN(I),EPS(NNN),YY(1,I,15),VV(1,I,15),(DISS(J,I),CF(J,I
```

```
     1),J=1,2)
 502 FORMAT(1H0,I5,3F10.4,2(F10.4,E15.4))
     IF(VERS.EQ.0.0) GO TO 48
C  METHOD OF MAPPING CONSTANT VELOCITY LINES BY ON LINE PRINTER
     DO 47 J=1,2
     DO 47 I=1,IA
     X(2)=0
     YYY(2)=ETA(J)
  11 DO 13 K=3,17
     X(K)=VV(J,I,K-2)
  13 YYY(K)=YY(J,I,K-2)
     X(1)=-X(3)
     YYY(1)=YYY(3)
     DO 39 II=1,12
     L=0
     XX=VELO(II)
     IF(XX.GT.X(17))GO TO 15
     DO 401 K=1,16
 401 IF(XX.GE.X(K).AND.XX.LE.X(K+1))L=K-2
     IF(L.LE.0) L=1
     IF(L.GT.13) L=13
     N=5
     IF(L.EQ.1) N=4
 402 COOR=POLINT(X,YYY,N,XX,L)
     GO TO 16
```

```
   15 COOR=YYY(17)
      WRITE(6,510)X(17),XX,I
  510 FORMAT(1H0,2F5.2,I5)
   16 DUMY=EXP(-COOR)
      CCOSH=(EXP(COOR)+DUMY)/2.
      SSINH=CCOSH-DUMY
      NNN=NN(I)
      XXL(KK)=-C*SSINH/(CCOSH+COS(EPS(NNN)))
      YYL(KK)=-XXL(KK)/SSINH*SIN(EPS(NNN))
      KK=KK+1
   39 IF(XX.GT.X(17)) GO TO 47
   47 CONTINUE
      KK=KK-1
      CALLPLOT3(YYL,XXL,KK,YMAX,YMIN,XMAX,XMIN,200,110,200)
   48 CONTINUE
      STOP
      END

$IBFTC VEL
      FUNCTION VEL(X)
      COMMON I,J,K,EPSM(180),EPS(180),EPSP(180),XS(2,25),YS(2,25),RADIUS
     1(25),YY(2,25,15),AR(2,15),CCOSH,PP(2,15),VV(2,25,15),Y(2,15),C,IA
      AL=.4*X*(1.-EXP(-X/26.))
      VEL=2./(1.+SQRT(1.+4.*AL*AL))
    2 RETURN
      END
```

```
$IBFTC AREA
      FUNCTION AREA(Z)
      COMMON I,J,K,EPSM(180),EPS(180),EPSP(180),XS(2,25),YS(2,25),RADIUS
     1(25),YY(2,25,15),AR(2,15),CCOSH,PP(2,15),VV(2,25,15),Y(2,15),C,IA
      EXTERNAL AREA1
      YY(J,IA,K)=Z
       DUM=EXP(-Z)
      CCOSH=(EXP(Z)+DUM)/2.
      AREA=GINTX4(AREA1,EPSM(I),EPSP(I))
      AR(J,K)=AREA
      IF(J.EQ.2)AREA=-AREA
      SINH=CCOSH-DUM
      XX=-C*SINH/(CCOSH+COS(EPS(I)))
      YX=-XX/SINH*SIN(EPS(I))
      Y(J,K)=RADIUS(IA)*ARSIN(SQRT((XX-XS(J,IA))**2+(YX-YS(J,IA))**2)/2.
     1/RADIUS(IA))*2.
      K=K+1
      RETURN
      END

$IBFTC AREA1
      FUNCTION AREA1(ZZ)
      COMMON I,J,K,EPSM(180),EPS(180),EPSP(180),XS(2,25),YS(2,25),RADIUS
     1(25),YY(2,25,15),AR(2,15),CCOSH,PP(2,15),VV(2,25,15),Y(2,15),C,IA
      AREA1=-1./(CCOSH+COS(ZZ))**2
```

```
      RETURN
      END
$IBFTC VOL
      FUNCTION VOL(Z)
      COMMON I,J,K,EPSM(180),EPS(180),EPSP(180),XS(2,25),YS(2,25),RADIUS
     1(25),YY(2,25,15),AR(2,15),CCOSH,PP(2,15),VV(2,25,15),Y(2,15),C,IA
      VOL=AR(J,K)*VV(J,IA,K)
      IF(J.EQ.2)VOL=-VOL
      K=K+1
      RETURN
      END
```

## 7.3 COMPUTER SOLUTION FOR THE POSITION OF MAXIMUM VELOCITY IN CONCENTRIC ANNULI

The position of maximum velocity in concentric annuli was found by Ivey, and Brighton and Jones to be dependent on radius ratio and independent of Reynolds Number and hydraulic diameter. The following programme was written to apply the present analysis to this simple case and predict the curves shown in Figure 16 and discussed in Section 4.

First the important FORTRAN symbols in the programme will be described.

| FORTRAN SYMBOL | DESCRIPTION |
|---|---|
| DPDZ | Axial pressure gradient, $\frac{dP}{dz}$ |
| F | Moody friction factor, f |
| G | Gravitational constant = 32.174, $g_c$ |
| RE | Reynolds Number, Re |
| RHO | Density, $\rho$ |
| RI | Inner wall radius, $r_i$ |
| RM | Turbulent flow location of maximum velocity, $r_m$ |
| RML(I) | Laminar flow location of maximum velocity, $r_{m\ell}$ |

| FORTRAN SYMBOL | DESCRIPTION |
|---|---|
| RO | Outer wall radius, $r_o$ |
| S(I) | Radius ratio, $s$ |
| SM(I) | Dimensionless radius of maximum velocity for turbulent flow, $\frac{r_m}{r_o}$ |
| SML(I) | Dimensionless radius of maximum velocity for laminar flow, $\frac{r_{ml}}{r_o}$ |
| TI | Inner wall shear stress, $\tau_{wi}$ |
| VIS | Kinematic viscosity, $\nu$ |
| VMI | Velocity at $r_m$ referenced to inner wall |
| VMO | Velocity at $r_m$ referenced to outer wall |
| TO | Outer wall shear stress, $\tau_{wo}$ |

The order of calculations in the programme listed in this section is as follows: Various radius ratios, the inner wall radius, the Reynolds Number, the kinematic viscosity, the gravitational constant and the density of the fluid are read in numerically. The friction factor is calculated from a linear approximation to the Moody diagram. For each radius ratio, the outer radius, the axial pressure gradient and the radius of maximum velocity for laminar flow are evaluated. With the initial estimate that the radius of maximum velocities for turbulent flow coincides with that for laminar flow, force balances on the two sections of the flow area divided by the line of maximum velocities yield the inner and outer wall shear stresses. Thus, two values of velocity may be calculated at the radius of maximum velocity using the asympotic form of the Van Driest velocity profile,

$$U^+ = \frac{1}{K} \ln Y^+ + C \quad .$$

The one velocity is referenced to the inner wall and the other to the outer wall. The two values of velocity are then matched by shifting the radius of maximum velocity in a trial and error procedure and repeating the calculations until the velocities agree to within 0.1 percent. This set of calculations is repeated for each radius ratio with the radius ratio, and the dimensionless radius of maximum velocity for

laminar and turbulent flow being printed out for each case.

```
      DIMENSION S(10),RML(10),SML(10),SM(10)
      READ(5,1)(S(I),I=1,9),RI
    1 FORMAT(10F8.3)
      READ(5,3)RE,VIS,G,RHO
    3 FORMAT(4F10.1)
      F=EXP(-0.2338*ALOG(RE)-1.34)
      DO 2 I=1,9
      RO=RI/S(I)
      DPDZ=F*(RE*6.*VIS/(RO-RI))**2/((RO-RI)*G/3.)*RHO
      RML(I)=SQRT((RO**2-RI**2)/(2.*ALOG(1./S(I))))
      SML(I)=RML(I)/RO
      RM=RML(I)
      L=1
    4 TI=DPDZ/2.*(RM**2-RI**2)/RI/12.
      TO=DPDZ/2.*(RO**2-RM**2)/RO/12.
      VI=SQRT(TI/RHO*G)
      VO=SQRT(TO/RHO*G)
      VMI=VI*(2.5*ALOG((RM-RI)/12.*VI/VIS)+5.5)
      VMO=VO*(2.5*ALOG((RO-RM)/12.*VO/VIS)+5.5)
      IF(ABS(VMI/VMO-1.).LE..001) GO TO 7
      IF(L.EQ.1) GO TO 5
      GO TO 6
    5 QI=VMI
      QO=VMO
```

```
      E=RM
      RM=RM-.005
      L=2
      GO TO 4
    6 SLI=(VMI-QI)/(RM-E)
      SLO=(VMO-QO)/(RM-E)
      BI=VMI-SLI*RM
      BO=VMO-SLO*RM
      RM=(BO-BI)/(SLI-SLO)
      L=L+1
      IF(L.GT.100)STOP
      GO TO 4
    7 SM(I)=RM/RO
      WRITE(6,8)S(I),SML(I),SM(I)
    8 FORMAT(3F10.4)
    2 CONTINUE
      STOP
      END
```

RESULTS

| $r_i/r_o$ | Laminar Flow $r_{ml}/r_o$ | Turbulent Flow $r_m/r_o$ |
|---|---|---|
| .05 | .408 | .237 |
| .10 | .464 | .329 |
| .15 | .508 | .399 |
| .25 | .582 | .509 |
| .30 | .615 | .556 |
| .40 | .667 | .638 |
| .50 | .736 | .711 |
| .60 | .792 | .777 |
| .70 | .845 | .838 |
| .80 | .898 | .895 |
| .90 | .950 | .949 |

## 8. REFERENCES


1. HEYDA, J. F.: "Heat Transfer in Turbulent Flow Through Non-Concentric Annuli Having Unequal Heat Release from the Walls", APEX-391, June, 1957.

2. VAN DRIEST, E. R.: "On Turbulent Flow Near a Wall", Paper No. 12, Heat Transfer and Fluid Mechanics Institute Symposium, University of California, Los Angeles, 1955.

3. DEISSLER, R. G. and M. F. TAYLOR: "Analysis of Fully Developed Turbulent Heat Transfer and Flow in an Annulus with Various Eccentricities", NACA-TN-3451, March, 1955.

4. DEISSLER, R. G. and M. F. TAYLOR, "Analysis of Turbulent Flow and Heat Transfer in Noncircular Passages", NACA-TN-4384.

5. BRIGHTON, J. A. and J. B. JONES: "Fully Developed Turbulent Flow in Annuli", Journal of Basic Engineering, pages 835-844, December, 1964.

6. IVEY, C. M: "The Position of Maximum Velocity in Annular Flow", Unpublished M.A.Sc. Thesis, University of Windsor, Windsor, Ontario, 1965.